SELF-ASSEMBLED LIPID BILAYERS FOR RAPID MEMBRANE SCREENING AND STIMULI-RESPONSIVE BIOMOLECULAR MATERIALS

by

ELIO JOSEPH CHALLITA

(Under the Direction of Eric Freeman and Donald Leo)

ABSTRACT

Cell membranes are complex nanostructures with remarkable properties. They are primarily composed of a lipid bilayer capable of hosting a multitude of biomolecules such as proteins, peptides, and pores that render the membrane stimuli-responsive and selectively permeable. Here, we exploit the inherent self-assembly properties of amphiphilic molecules found in cell membranes to develop 1) membrane-based stimuli-responsive materials and 2) novel micromembrane electrodes for biomolecular sensing. To this end, we use the droplet interface bilayer (DIB) technique that consists of creating synthetic bilayers at the interfaces of aqueous droplets in oil. We develop a droplet printer to print large networks of interconnected droplets at a much larger scale than previously feasible. The resulting tissue-like material is then encapsulated in a thermosensitive organogel to improve its portability, durability, and practicality in non-laboratory settings. We also propose novel hydrogel-based electrodes to create aqueous-hydrogel micromembranes in oil using similar self-assembly techniques, rapidly forming and separating lipid membranes for determining droplet compositions. Both topics demonstrate the potential for membrane-based materials and the use of lipid membranes in biomolecular detection.

INDEX WORDS: Lipid bilayer membranes, Droplet interface bilayer, 3D Printing, Biomolecular smart materials, Microfluidics, Screening

SELF-ASSEMBLED LIPID BILAYERS FOR RAPID MEMBRANE SCREENING AND STIMULI-RESPONSIVE BIOMOLECULAR MATERIALS

by

ELIO JOSEPH CHALLITA

B.E., Mechanical Engineering, Lebanese American University, Byblos, Lebanon, 2015

A THESIS Submitted to the Graduate Faculty of The University of Georgia in Partial Fulfillment of the Requirements for the Degree

MASTER OF SCIENCE

ATHENS, GEORGIA

201

SELF-ASSEMBLED LIPID BILAYERS FOR RAPID MEMBRANE SCREENING AND STIMULI-RESPONSIVE BIOMOLECULAR MATERIALS

by

ELIO JOSEPH CHALLITA

Major Professors:	Eric Freeman Donald Leo
Committee:	Leidong Mao R. Benjamin Davis

Electronic Version Approved:

Suzanne Barbour
Dean of the Graduate School
The University of Georgia
August 2018

TABLE OF CONTENTS

Page

LIST OF TABLES

Page

LIST OF FIGURES

Page

CHAPTER 1

INTRODUCTION

1.1. Cell Membranes

The ability of modern cellular life to evolve from its rudimentary structure was contingent upon biological membranes. This allows the creation and maintenance of an independent microenvironment shielded from the outside world where genetic, metabolic and other complex biological processes can thrive (Figure 1). Cell membranes define, separate and protect the intracellular space of cellular organisms from their extracellular surroundings. They are essential and complex structures in prokaryotic and eukaryotic cells. Not only do they act as barrier, they are also selectively permeable: they manage the passage of species across it, thus playing a central role in signal transduction and information processing among cells and their surroundings [1].

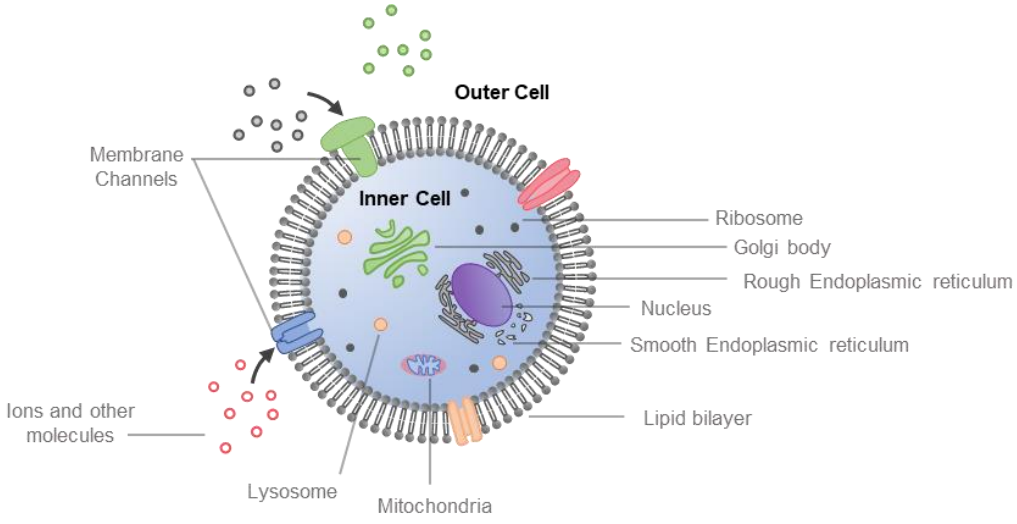

Figure 1- Simplified representation of a Cell – Organelles reside inside the cytosol (interior of the cell) which is separated by a lipid bilayer from the outer environment

1.2. Functional Properties of Cell membranes

1.2.1. Selective permeability and stimuli-responsive functionality

A cell membrane generally consists of a lipid bilayer formed by two opposing leaflets predominantly composed of tightly-packed phospholipids. However, other biomolecules such as proteins may also reside on or within the membrane. Phospholipid bilayers form a near-impermeable seal that prevents the transport of various substances and species from and into the cellular interior. The selective permeability of the membranes, however, is facilitated by transport proteins and peptides such as channels, pumps and pores that play an important role in passively or actively transporting various species across the membrane.

These transport proteins and peptides are often stimuli-responsive. Once triggered by an external stimulus, they change their structural conformation to allow the exclusive flow of specific molecules such as cations and anions. External stimuli may be classified as chemical, optical, mechanical and electrical in nature [2]. For instance, bacteriorhodopsin (bP) proteins are light-driven photon pumps used by *Archea* that capture light to move protons out of the cellular space [3]. Alternatively, Large Conductance Mechanosensitive Ion Channels (MscL) are mechanically-activated proteins that may be found on the plasma membranes of *Escherichia coli* bacteria [4]. They help saving the bacteria undergoing hypo-osmotic stress from lysis by allowing ion to move across the membrane, by responding to membrane strain.

1.2.2. Mechanical and materials properties

From a structural standpoint, cell membranes are thin (~ 5-10 nm in thickness), dynamic and fluid-like structures [5]. At this scale, forces such as the Van der Waal forces, hydrophobic interaction, steric interactions, and electric double layer interactions are dominant [6]. As a result,

lipids are free to move resulting in flexible yet robust membranes: they can bend, morph and stretch as they seek a new structural equilibrium in response to external mechanical perturbation.

Similar to other biological systems, the structure of cell membranes determines their function. Changing the composition of the lipid bilayer highly affects its mechanical and materials properties such as elasticity, bending modulus, fluidity and thickness [7-11]. For instance, increasing the cholesterol to phospholipids ratio (C/PL) in the plasma membrane decreases its fluidity and permeability and changes its stiffness [9, 10].

Temperature also affects the fluidity and the physical state of the membranes. Below a threshold temperature called transition temperature T_c, specific to bilayer, the liquid-crystalline membrane changes into a viscous gel state [6]. This loss in fluidity impedes biological reactions and processes at the membrane and makes the membrane more prone to rupture. However, some organisms living in relatively extreme environments have developed cell membranes highly adaptable to large fluctuations in temperatures. Cell membranes found in wood frogs are able to survive multiple freeze and thaw cycle without significant changes in the membranes' structure and function [12]. Moreover, some plasma membranes possess self-healing capabilities. For example, the plasma membrane of *Xenopus* oocytes can spontaneously self-repair in the event of ruptures and tears at the bilayer-level [13].

1.2.3. Self-assembly and organization of membranes

Lipids are the main components of an animal cell membrane. They constitute around 50% of mass of the cell membrane with the rest mostly being proteins [14]. All lipids found in cell membranes are amphiphilic molecules - meaning they have a hydrophobic ("water-fearing") side and a hydrophilic side ("water-loving") side. Once dissolved, lipid molecules aggregate and form various mesoscopic structures depending on their size, type, chemical composition and the type of

solvent used (Figure 2). Both attractive and repulsive forces, also dubbed as the *Hydrophobic Effect*, drive the self-assembly of the amphiphilic molecules into organized structures [15, 16].

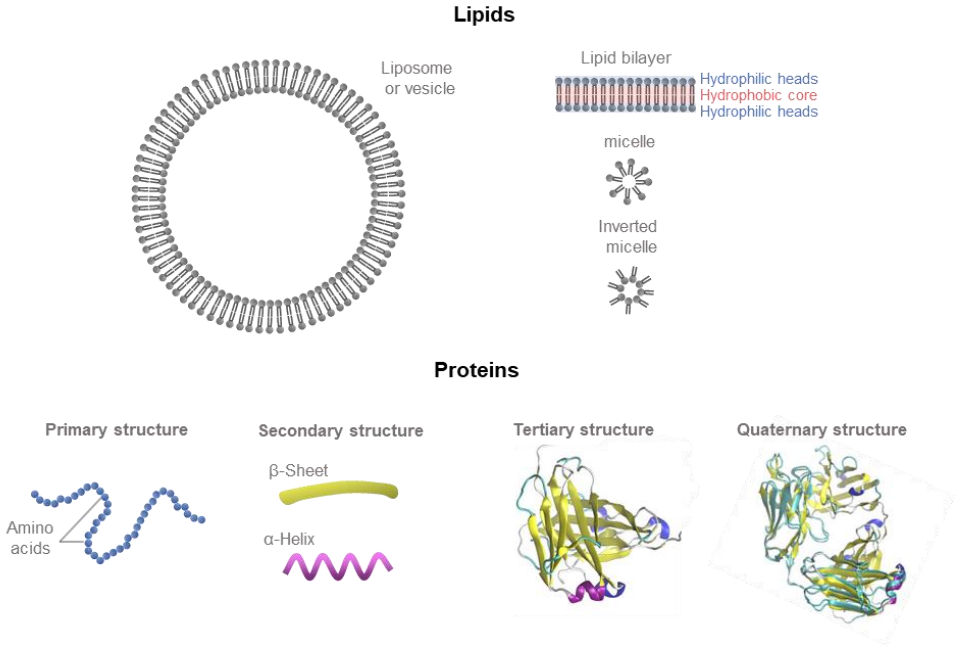

Figure 2 - Self-assembly of lipids and protein into large structures – Phospholipids may assemble into various shape due to their hydrophobic tails and hydrophilic heads. Alternatively, proteins fold into various confirmation with multiple structures.

The self-assembly principles also apply to membrane proteins, peptides and pores. Structurally, proteins are large molecules composed of a chain of connected amino acids that fold into unique 3D arrangements called tertiary structures (peptides consist of ≤ 50 A.A.). They could spontaneously bind, insert or even span across the membrane (integral proteins) through its hydrophobic core. Some membrane proteins such as the alpha hemolysin (αHL) pore may also form aggregates creating quarterly structures in the membrane to pursue its functions.

1.3. Cell membranes as novel biomolecular smart materials

The multifunctional capabilities of cell membranes inspire the creation of novel membrane-based active materials and devices for engineering applications [2]. The biomolecular material could be mainly controlled by regulating the transport across the cell membranes. This is facilitated by the stimuli-responsive nature of most of the proteins that reside in the membrane. Similar to traditional and engineered smart materials such as piezoelectric ceramics, ionic polymer transducers, and shape memory alloys, the biomolecular material may couple between different physical domains. Moreover, cell membranes may host a multitude of protein channels at the same time, each of them being responsive to stimuli of different nature [17] – a property seldom found in traditionally engineered active materials (Figure 3). In addition, given the structure-function relationship of protein with the emergence of genetic engineering, the amino acid sequence (the building block of proteins) could be tailored to achieve a myriad of tertiary and quarterly protein structures. This may result in a new class of engineered proteins that do not necessarily mimic naturally occurring ones but could also possess unparalleled functionalities.

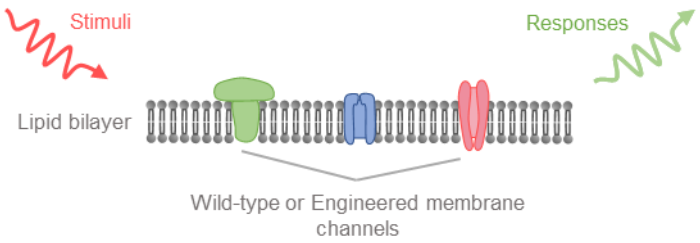

Figure 3 - Stimuli-responsive membrane channels embedded in the membrane.

In addition, the flexibility of membranes due to their fluid-like structure renders the material mechanically dynamic rather static. This gives the material the ability to change shape to

a certain extent, in response to mechanical force as it search for a new equilibrium without breaking or failing [18]. Morphing and shape changing materials are important for applications such as soft robotics [19, 20].

The self-assembly properties of biological membranes coupled with their flexibility and multifunctionality gives them a unique advantage over traditional smart materials. However, cell membranes remain challenging entities due to their complex structures where a numerous biomolecular interactions take place and the difficulties to maintain their native physiological settings [21]. While their fundamental components are well understood, the precise composition of biological membranes in a cell remains quite elusive.

Model membranes may be employed to understand the composition, structure and functions of biological membranes [22]. They are a simplified replicates of cell membranes in terms of structures and composition, making experiments and physiological studies of cell membranes more controllable.

1.4. Model Membranes

Cellular membranes have long been a subject of scrutiny by scientist and engineers. The challenges with the investigation of complex physiological phenomena involving cell membranes may be partially addressed by faithfully replicating them in a controlled environment. Model membranes are synthetic and simplified analogues to cell membranes. Their purpose is to reproduce and more importantly isolate certain aspects of the membrane's structures and functions for a more precise and detailed examination. Model membranes have been implemented in a various studies to understand concepts such as membrane-drug relationships [23], interactions of peripheral membranes proteins with lipids [24], ion channel activities [25], and the membranes'

bending rigidity [7]. This approach allows for insights into the overall properties and functionalities of the cellular boundaries.

Moreover, model membranes are suitable for bottom-up synthetic biology. Owing to their simplicity and ability to reconstitute specific stimuli-responsive biomolecules, model membranes are minimal structures that can mimic specific and intricate cellular functionalities. They provide better control on the composition and structure of membranes to achieve desired functionalities with great precision. For this reason, they may be used to design membrane-based active materials with specific functionalities. For instance, model membranes have been used to create osmotic actuators [26], hair-like sensors [27] and biobatteries [28] .

Several approaches have been devised to the development of synthetic analogues of cellular membranes. Each of these techniques take advantage of the amphiphilic properties of the lipids and proteins during the self-assembly process. The most common model membranes are lipid vesicles (or liposomes), lipid monolayers, and supported lipid bilayers.

1.4.1. Lipid vesicles (liposomes)

Lipid vesicles are spherical-shaped lipid bilayers (Figure 4). They enclose a small aqueous compartment of various sizes with diameters ranging from as little as tens of nanometers for small unilamellar vesicles (SUVs) to a large as tens of micrometers for giant unilamellar vesicles (GUVs) – the closest in size to cells [29, 30].

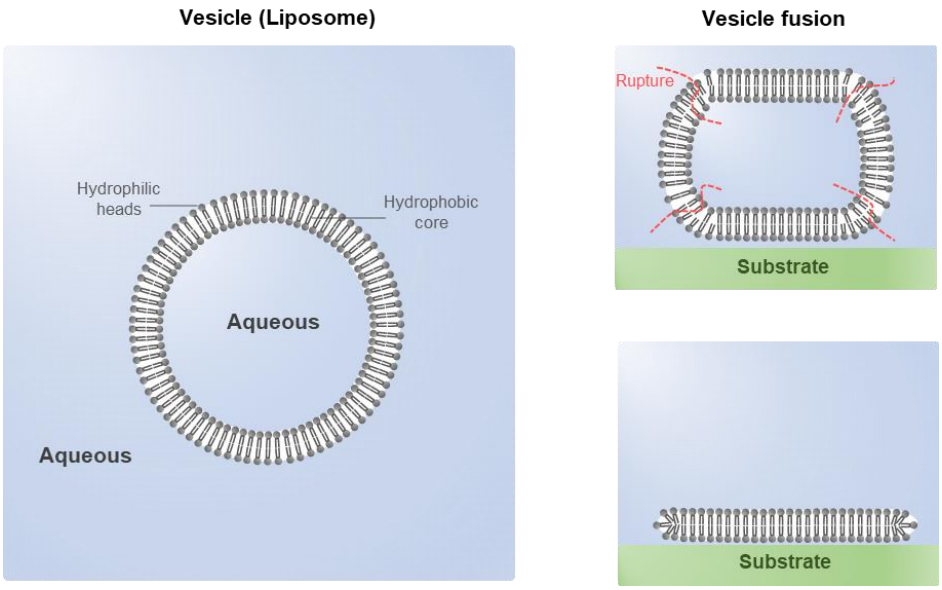

Figure 4 – Vesicles are formed after being dissolved in an organic solvent such as chloroform which is subsequently evaporated. This forms a dry thin film of lipids which is later mixed with an aqueous solution to drive the self-assembly of the lipids into the vesicles. These vesicles could be sonicated or filtered to make them more uniform in size. Vesicle fusion happens after the introduction of the vesicle in a dish containing a supporting substrate such as mica, gold, or glass.

Vesicles, also called liposomes, may be created from a lipid-aqueous solution. The latter may be extruded through a membrane containing pores of specific sizes. Alternatively, the mixture could be sonicated while changing the power and time of sonication to achieve desired vesicle dimensions. However, the challenge lies in the reconstitution of membrane proteins into vesicles due to the evaporation step usually required during their preparation [30]. Several methods have been developed to solve this problem including electroformation [7, 31] or improving the stability of proteins using sucrose [32]. In addition, vesicles could be fused to a supported lipid bilayer or to solid surface such as glass, mica or gold. As it reaches the substrate, the vesicle ruptures and forms flakes that either form a bilayer or deliver specific biomolecules to pre-existing bilayers [33, 34] (Figure 4).

1.4.2. Lipid monolayers

A lipid monolayer is one leaflet of the lipid bilayer. Similar to bilayers, it may be self-assembled spontaneously owing to the *hydrophobic effect*. It is a single molecule thick membrane formed on the surface of an aqueous phase. It is often called a Langmuir monolayer and may be studied using a Langmuir-Blodgett trough, in which variables such as lipid composition, subphase and temperature could be tuned to resemble biological settings [29, 35, 36].

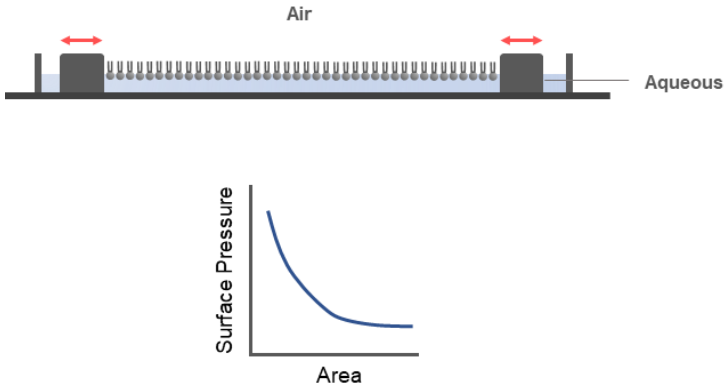

Figure 5 - One way to create and study lipid monolayer at the water-air interface is through a Langmuir trough. This used to compress or decompress the thin lipid film on a given subphase using a sliding solid barrier. As a result the surface pressure increases as the film area (or area per molecule) decreases and the lipids aggregate.

Lipid monolayers are simplified model membranes possessing a relatively stable and homogenous 2D planar geometry. They are typically used to study the interaction of drugs with lipid membranes [37], lipid-lipid interactions [38] and drug delivery systems [23]. Lipid monolayers may be even used to reconstitute and study membrane proteins and peptides at the water-air interface [39, 40] such as bacteriorhodopsin [41] and aliphatic peptide gramicidin [42].

1.4.3. Supported and tethered lipid bilayers

Surface supported lipid bilayers (SLBs) are planar model membranes supported by a solid such as mica, glass, SiO2 or modified gold surfaces properties [39] (Figure 6). SLBs could be fabricated using different methods including vesicle fusion [11]. Unlike Langmuir monolayers, SLBs are closer to biological membranes in terms of structure and may hold key functions found in cells. However, one part of the hydrophilic headgroups is firmly adhered to the supporting surface affecting their fluidity of the membrane and limiting any control over their alignment. These factors are important especially when studying integral proteins channels which may not be able to span across the membrane [39] .

These problems have been addressed by developing tethered bilayer membranes (t-BLM) whereby “spacer molecules” could be introduced between the lipid bilayer and the solid surface. Another method includes separating the lipid bilayer from the solid surface using hydrated polymers that act as a soft cushion. These solutions allow the lateral movement of membranes with any restrictions and prevent the unwanted interactions between components in the membranes such as membrane proteins with solid substrate. Furthermore, it would ensure the stability and sturdiness of theses system for various biosensor applications [43], and membrane-drug interactions [44].

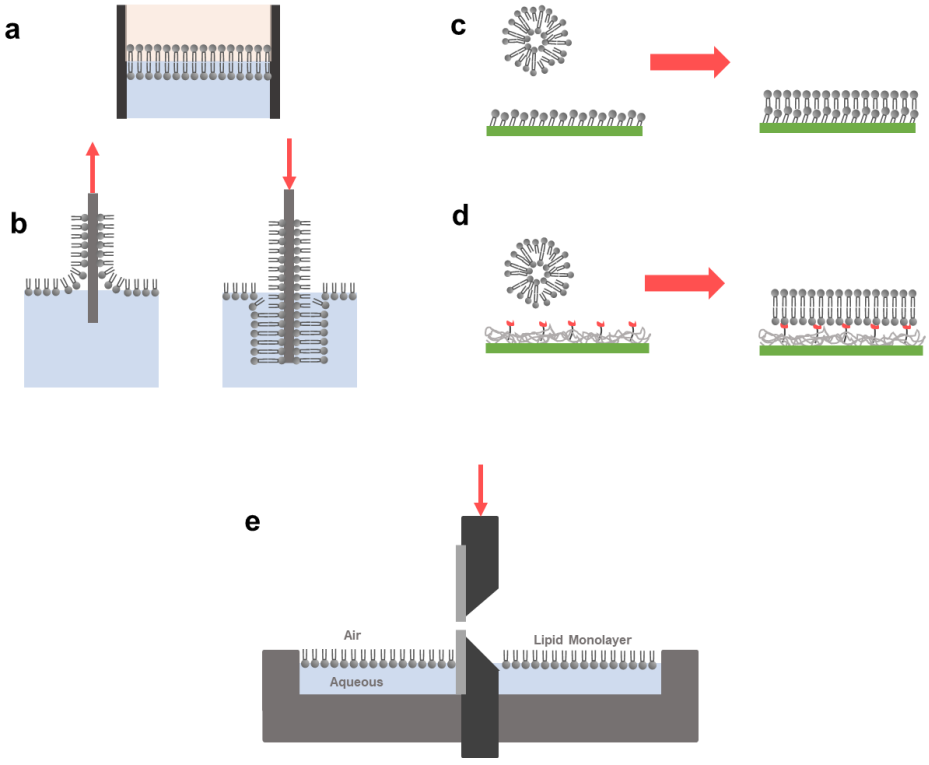

Figure 6 - Supported and tethered lipid bilayers. a) Black lipid membrane (BLM) formed at the interface of two immiscible aqueous phases b) The Langmuir-Blogett method used to move one or more layers of lipids into a solid substrate c) Self-assembled monolayers (SAM) which are covalently bonded to a solid support. They could attach to other lipid layers by vesicle fusion. d) Cushion created by a layer of polymer coating tethered on a surface of solid support. They could attach to lipid bilayers that form due to vesicle fusion substrate e) Montal-mueller technique where two electrolyte solutions are separated by hydrophobic septum. Lipid monolayer are formed at the water-air interface in this case may be used to create a bilayer by increasing the volume of the electrolytes.

Other supported membranes include the Montal-Mueller (MM) technique (Figure 6) which is one of the earliest methods developed to create synthetic membrane [45]. It consists of two electrolyte solutions separated by a hydrophobic septum, typically prepared from Teflon or silicone. The phospholipids are mixed with chloroform and ethanol and are introduced at the surface of the electrolyte. Therefore, a lipid monolayer spontaneously forms at the water-air interface. When the level of the electrolyte solution is elevated, a bilayer forms at the septum.

Since the chloroform or ethanol employed to cover the electrolyte solution evaporates, the subsequent bilayer is considered solvent free [46].

1.5. Droplet interface bilayer (DIB) and droplet hydrogel bilayer (DHB)

Recently, the droplet interface bilayer (DIB) technique has emerged as a powerful tool to form robust and stable synthetic lipid bilayers for various physiological studies. The DIB method also relies on the self-assembly principles of the amphiphilic components of cell membrane. A synthetic lipid bilayer may be formed at the conjoining interface of a pair of lipid encased aqueous droplets in an oil medium [25] (Figure 7). As the lipid coated droplets get closer to each to other, the monolayers gradually zip and expel the intervening oil before forming a bilayer. A DIB could be formed, separated then reformed several times. Unlike other model membranes, DIBs are entirely fluidic whereby aqueous droplets act as a scaffold that support the lipid bilayer. However, water swollen hydrogel-droplets have been shown to form lipid bilayers at their fluidic interfaces [47]. Also, DIBs last longer and can stay functional for a time range of few days to few months [25].

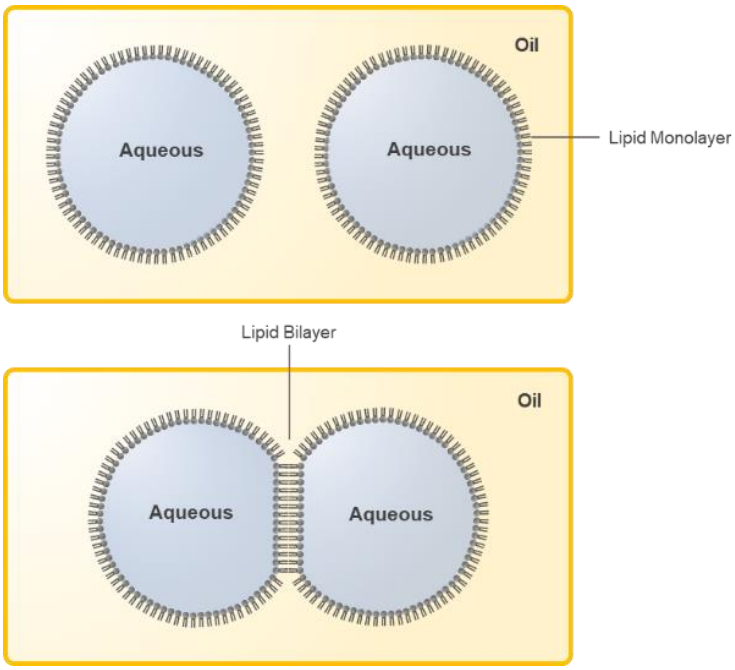

Figure 7 - Droplet interface bilayer technique consists of forming a lipid bilayer at the intersection of a pair of lipid encased aqueous droplets in oil.

Another interesting aspect of DIBs is their capability to host a large variety of transmembrane proteins and peptides [25, 48]. In fact, they have been implemented to study various stimuli-responsive membrane proteins such as the mechanosensitive channel MscL [4, 49], proton-pump bacteriorhodopsin (bR) [3, 50], voltage-sensitive peptide Alamethicin (Al) [47, 51, 52] and alpha-hemolysin pores (αHL) [53, 54].

During DIB preparation, lipids molecules could be introduced in the oil phase ("lipids-out") or in the aqueous phase ("lipids-in"). In both methods, lipids self-assemble into a lipid monolayer at the water-oil interface albeit with a different incubation time that range from few second to > 30 min depending on the droplet size, buffer components, oil type and type of amphiphile. In the lipids-out technique, all the droplets share the same lipid composition. However,

one important feature of the lipids-in technique is the ability to create asymmetric durable lipid bilayers which are more common in biological membranes [55].

Planar bilayers may also be formed between lipid encased droplets and surfaces that could accommodate the self-assembly of lipids in oil. For instance, the droplet may be brought down to sit on top of the lipid coated hydrogel forming a droplet-on-hydrogel bilayer (DHB) (Figure 8). DHBs have been used to mechanically gate MscL in the membrane by systematically injecting nanoliter volumes in the droplet [56] and to study the membrane capacitance by regulating the membrane area [57].

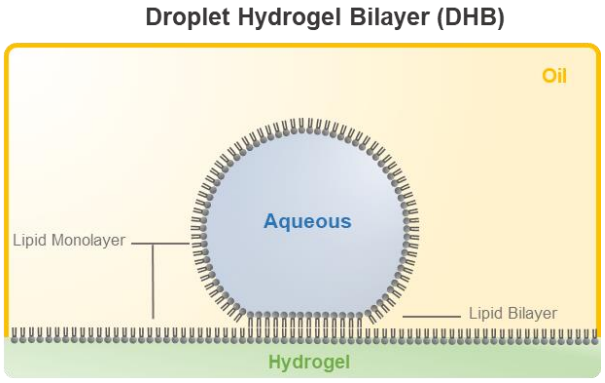

Figure 8 - Droplet hydrogel bilayer – A lipid bilayer may be formed between a droplet and a hydrogel-infused solid substrate.

1.6. Electrical model of droplet interface bilayers

A lipid bilayer is a near-impermeable barriers that prevents the transport of ions and other species across it. At the same time, its ability to host stimuli-responsive membrane proteins and peptides such as channels, pumps and pores render it selectively permeable.

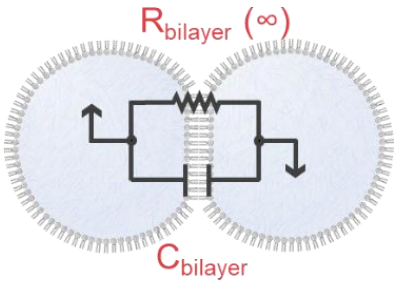

Figure 9 - Electrical Model of a lipid bilayer which consists of a large resistor and a capacitance in parallel

Electrically, a pure lipid bilayer may be approximated as a capacitor in parallel with a large resistor as shown in Figure 9. (Specific resistance of ~10MΩ·cm^2 for 1,2-diphytanoyl-*sn*-glycero-3-phosphocholine DPhPC lipids) [6, 8, 47, 58]. In this model, the resistance R of the membrane is related to its permeability to ions, whereas, the capacitance C_M is related to the area A_M, thickness d, and permittivity $\varepsilon_0\varepsilon_r$, and is given by the following equation:

$$C_M = A_M \frac{\varepsilon_0 \varepsilon_r}{d} \tag{1}$$

The total ionic current across the membrane is a combination of a resistive (I_R) and capacitive (I_C) components. The total current is predicted by the following equation dependent on the voltage V:

$$I = I_C + I_R = C_M \frac{dV}{dt} + \frac{V}{R} \tag{2}$$

Because lipid bilayers tend to have low permeability to ions, the resistive component of the ionic current is considered negligible ($R \rightarrow \infty$, $I_R \rightarrow 0$). Adding membrane proteins and peptides, however, changes the permeability and with it the resistivity of the membrane. In this case, the

equivalent conductance ($\frac{1}{R}$) of the membrane corresponds to that of the membrane proteins and the resistive component is no longer negligible.

1.7. Networks of Droplet interface bilayers

One critical feature of DIBs is their scalability. Lipid bilayers in the DIB platform possess adhesive forces strong enough to anchor adjacent aqueous droplets and prevent their separation. This allows the assembly of multiple lipid encased droplets together in oil into large and complex 2D and 3D structures of interconnected droplets [59, 60]. In these networks, every droplet represents an independent compartment which may hold a distinctive internal content. Similar to tissues, these compartments are able to cooperate and exchange information with their neighboring droplets across the lipid bilayers which may be functionalized with membrane proteins [60]. This gives rise to emergent functionalities that are not found in aggregates of independent and separated droplets [61].

This important aspect gives DIBs a unique advantage over other artificial bilayer platforms for the creation of membrane-based active materials. While vesicles (liposomes) are the most structurally similar to cells, they are inherently not capable of aggregating into large connected clusters without the need of specialized proteins such as gap junctions [62, 63].

DIB networks have been used to fabricate microdevices for various engineering applications. For example, by introducing a concentration gradient within specific droplets within the DIB network, Villar *et al.* created folding 2D and 3D structure that may act like osmotic actuators [63] . In addition, the incorporation of membrane proteins and pores in specific droplets within 2D DIB networks have also been used to create bioelectronic devices such as a full-wave rectifier [60], a biobattery [64] and a NAND logic gate [65]. A conductive pathway within a large

3D network of DIBs have been produced by incorporating αHL pores in these droplets [63] which may also be turned ON by an external stimulus such as UV light [3]. Owing to their simplicity, energy-coupling abilities and functional versatility, DIBs have been proposed as building blocks for membrane-based stimuli-responsive materials for engineering applications including sensing [4, 27], actuation [26] and energy harvesting [28].

It is evident that networks of DIBs offer more than what single lipid bilayer formed between a pair of droplet offers. In fact, networks of DIBs have promising applications in the fields biotechnology, medicine and smart material systems [59]. Recently, the reconfiguration of networks of DIBs was achieved by the selective ruptures of specific membranes within large networks of DIBs. This caused the entire networks to shift, bed and morph into a new shape which corresponds to a new equilibrium [66].

1.8. Objectives

The work presented in this thesis provides the following advancements:

1- **The realization of biomolecular stimuli-responsive materials inspired from cell membranes and tissues.**

2- **Development of a novel model membrane technique for rapid membrane screening.**

The fundamental components implemented in both topics are the self-assembly principles found in biological cell membranes. The next chapters will introduce a novel droplet printing method for the fabrication of networks of DIBs. Furthermore, we will advance their portability, durability and functionality of these networks by encapsulating them in a thermosensitive organogel. In addition, a hydrogel-based electrode is developed for rapid screening of lipid membranes. The novel electrode is inspired by DIBs and DHBs and offers a powerful method to detect the internal components of droplets.

CHAPTER 2

BIOMOLECULAR STIMULI-RESPONSIVE MATERIALS[1]

2.1. Constructing droplet interface bilayer networks

The most common approach for constructing DIBs involves hand-pipetting aqueous droplets in oil then manually manipulating them into contact. While this technique is suitable for studying single membranes or smaller aggregates of droplets, it is not efficient for creating large DIB networks. To overcome this limitation, several active and passive techniques have been developed to form 2D and 3D DIB networks which may rely on heating using a laser [69, 70], dielectrophoresis [71], electrowetting [72] or using microfluidic droplet generators [73-75]. Nonetheless, these methods are restricted as they do not allow the rapid creation of well-defined DIB networks' architecture or are intrinsically limited by the microfluidic chip [67]. Recently, Villar *et al.* from the Bayley group in Oxford, developed a piezoelectric-based 3D droplet printer capable of printing thousands of droplets of well-defined architectures. The printer is similar to other drop-on-demand technologies and is able to produces consistent droplets in oil having a smaller than the nozzle diameter (<100 μm) with different internal components [59, 63, 67]

[1] This chapter is a modified and shorter version of the work published in 67. Challita, E.J., et al. *A 3D printing method for droplet-based biomolecular materials*. in *SPIE Smart Structures and Materials + Nondestructive Evaluation and Health Monitoring*. 2017. SPIE. And 68. Challita, E.J., et al., *Encapsulating Networks of Droplet Interface Bilayers in a Thermoreversible Organogel.* Scientific Reports, 2018. **8**(1): p. 6494.

2.2. Pneumatic-based droplet printing apparatus

In this work, we develop a novel droplet printing technique for the creation of 2D and 3D structures of droplets connected by lipid bilayers in an oil-rich environment. The printer is capable of generating droplets as small as 50 μm and as large as 1 mm in diameter at a rate of a droplet every 5 seconds. The following sections will describe the printing setup as well as the steps usually taken before and during the printing process.

2.2.1. Setup

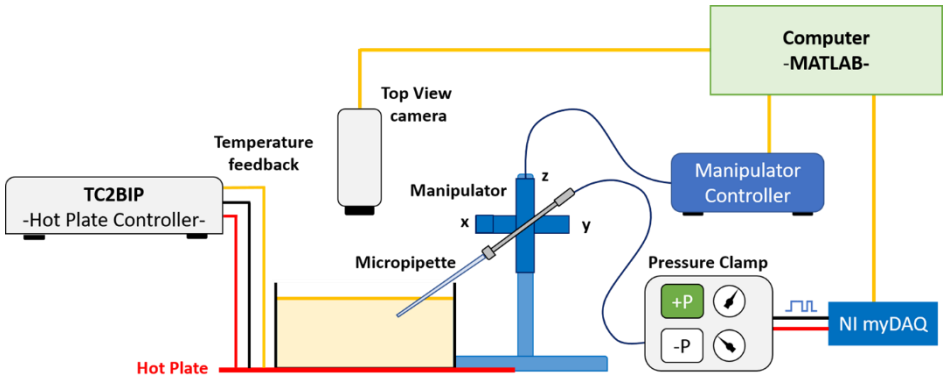

Figure 10 - Pneumatic-based droplet printer from [68].

The printing setup shown in Figure 10 has three main components:

- Glass micropipette filled with the desired aqueous solution
- Pressure supply
- Micromanipulator

The glass capillary is pulled to a fine point using a pipette puller (Shutter instrument p-1000), allowing for the creation of glass needles from capillaries. This pulled glass capillary is filled with the desired aqueous solution using a microfil and then connected to the pressure supply via silicone tubing. To control the needle location for droplet ejection, the micropipette is mounted

on a computer-controlled 3-axis manipulator. In this setup, the micropipette is tilted to a 30° angle to prevent it from obstructing the view from the microscope.

A high-speed pressure clamp (HSPC, ALA Scientific) controlled by an NI-myDAQ is used to apply pressure to the aqueous column inside the micropipette. However, other pressure sources such as the Eppendorf femtojet microinjector may be used [67]. During printing, the NI-myDAQ sends a series of discrete voltage signals of specific amplitudes and durations to the HSPC. The latter translates the signal into a sequence of pressures in the glass capillary to inflate the microdroplet at the tip of the micropipette. The micromanipulator and pressure supply are synchronized by a MATLAB code. A zoom microscope with a CCD camera is used to monitor the printing process and provide feedback on the creation of the networks.

2.2.2. Printing Methodology

The printing methodology consists of two steps: 1) moving the micropipette to its exact location using the automated micromanipulator and 2) generating the droplet before snapping it off the tip of the pipette. The shape and geometry of the desired droplet network is provided by the user by filling an Excel sheet (Figure 11). The sheet contains specific cells that are organized in a rectangular coordinate-like system initially filled with zeros. The user changes specific cells to one to specify the existence of a droplet or keeps it zero to indicate otherwise. Once done, a MATLAB script scans the Excel sheet and extracts the x-y coordinates of each droplet. These coordinates are subsequently multiplied by correction factor found in a calibration step [67] that precedes the printing of the network to get the true coordinates of the droplets.

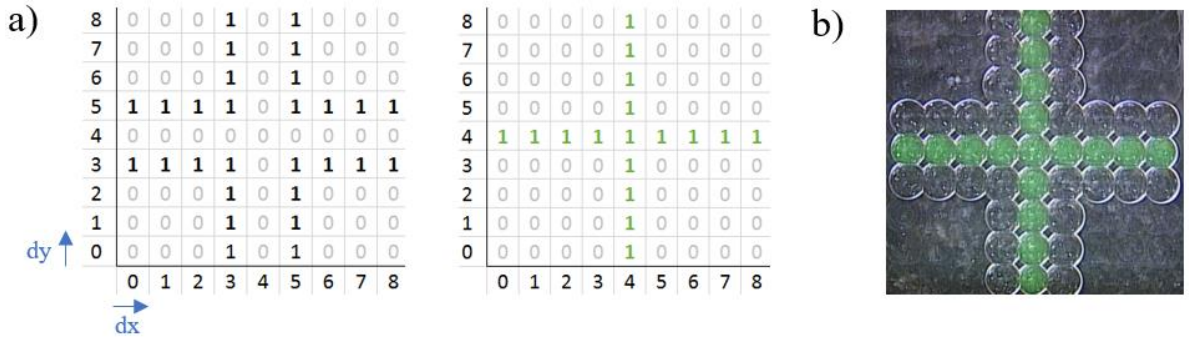

Figure 11 - DIB networks layout in an Excel sheet. In this layout, two different solutions were used to print this pattern. Therefore, the Excel sheet is updated after the first iteration and another needle containing the second solution is used.

During the calibration step, the correction factor is set equal to the average diameter of the injected droplets (N=50) measured visually in a separate dish. This distance is found to be both adequate to form bilayers between adjacent droplets and nondisruptive to the already established DIB structures that may be otherwise disrupted by the falling droplets. Next, the printing area is specified in another printing dish containing the same oil mixture, by setting the reference points X_0 and Y_0 equal to zero, and Z_0 equal to around 400 microns below the meniscus level. At this point, the printing may be initiated.

During printing, once the micropipette reaches its predefined location, pressure is applied to the aqueous solution and a microdroplet is formed at the tip of the micropipette. Subsequently, the micromanipulator is moved outside the oil phase into the air to detach the droplet from the micropipette by the surface tension of the meniscus (Figure 12). As the droplet falls within the oil solution, lipid molecules present in either the oil or aqueous phases self-organize at the droplet surface and form a monolayer. Once it reaches the bottom of the dish, the lipid-coated droplet forms bilayers with adjacent droplets at their points of intersections.

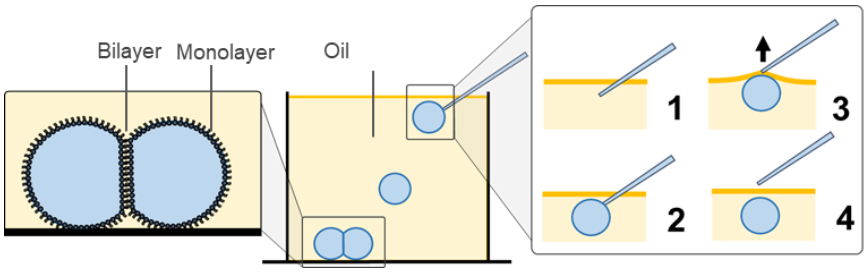

Figure 12 - Printing aqueous droplets in an oil reservoir. Once formed at the tip of the printing needle, a droplet is released by the capillary forces of the meniscus as the needle is pulled outside the oil phase. A lipid monolayer forms around the falling droplets. Once they reach the bottom, the lipid encased droplets form bilayer with other adjacent droplets.

The droplet printer may also generate droplets having different internal contents. This allows the creation of droplet networks of various functionalities. In this case, swapping the glass capillary with another containing the desired solution is necessary between iterations.

2.2.3. Printing large 3D DIB networks

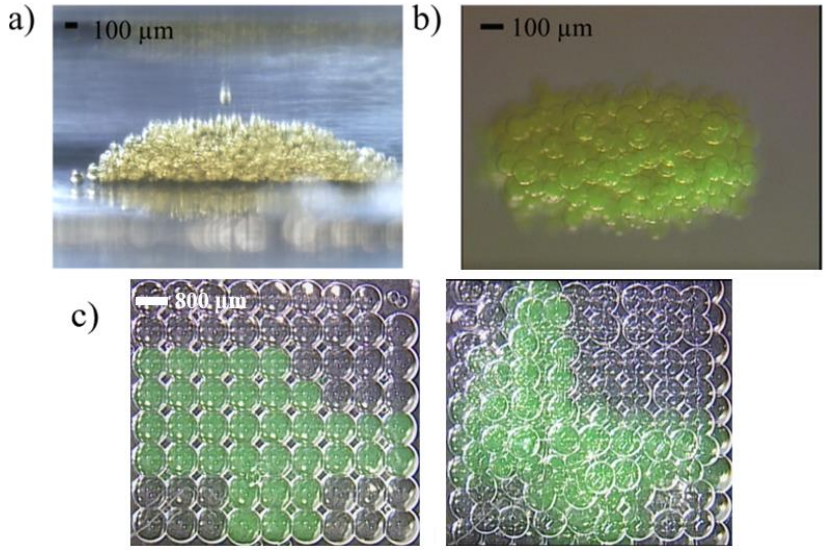

Figure 13 - Printed Network of DIBs. a) a 3x10 printed network of DIBs. Droplets may fall down at the edges, creating a trapezoid-like shape b) droplets printed on a create substrate to enforce a rectangular shaped layout.

Large 3D structures of DIBs may also be constructed in this fashion. In this case, the droplets would be printed layer by layer. Lipid bilayers in the bottom layers are strong enough to

support thousands of droplets without separating [63]. Moreover, the geometry of each of the upper layers may be iteratively changed in the Excel sheet as the printing progresses as shown in Figure 13.

However, droplets near the edge of the structure may not settle down in their printed location and may roll down due to gravity (Figure 13.a). For instance, printing a 3-by-10 rectangular prism results in a trapezoidal prism-like profile as shown in Figure 13.a. This is due to the period of time between initial droplet-droplet contact and bilayer formation. These effects become more pronounced as the size of the droplets increase.

DIB networks may also be functionalized with transmembrane proteins and peptides. For instance, alpha hemolysin (αHL) pores may be introduced in specific droplets within the network to create a conductive path within an otherwise insulating network [59, 63, 67]. Upon the application of a DC voltage between the droplets containing the pores, ions flow from one compartment to another generating a nonzero ionic current response between the electrodes (Figure 14).

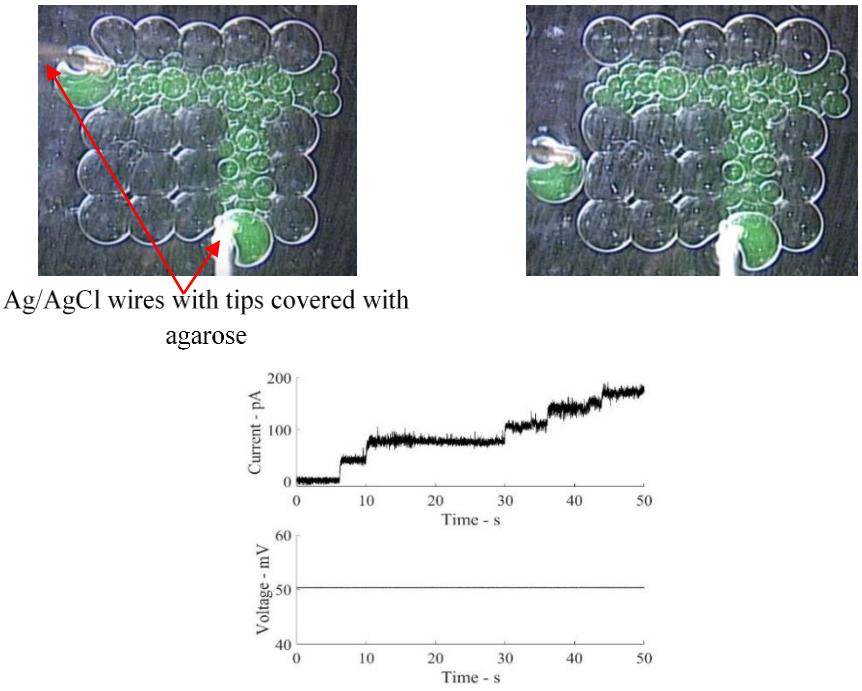

Figure 14 - Networks of DIBs with a selective pathway containing aHL pores. a) Measurement are taken between the stacked green droplets that contain the aHL pores b) They are compared to the measurement across an isolating part of the network c) Step-wise increase sue to current due to aHL insertion in part a) while no change in the current is observed in part b)

2.2.5. Drawbacks and proposed solutions

DIB networks are delicate due to their fluid-in-fluid structure. This property restricts their usage outside the laboratory environment. Several attempts have been made to overcome this challenge including confinement of the droplets in a solid substrate [52] or in microfluidic devices [51]. These designs consist of an oil inclusion within a solid-matrix and do not necessarily stabilize the droplets themselves. This renders these attempts static in the sense that once encapsulated, access to the droplets is restricted and reconfiguration is not feasible without creating a new substrate. Also, such methods allow limited control on the design of large networks of droplets with specific 3D architecture.

Venkatesan *et al.* tackled this problem by mixing the hexadecane oil phase with low concentrations of Poly(styrene-b-ethylene-co-butylene-b-styrene) (SEBS). The resulting mixture is a thermosensitive organogel that is solid at room temperature and may transforms into a viscous liquid at higher temperatures. They proved that this mixture could be used to stabilize and encapsulate single DIBs without affecting their capability to host functional membrane peptides such as Alamethicin [17].

Encapsulation of the bilayer membranes could also be achieved in hydrogel which may play an additional role in bottom-up synthetic biology. For instance, hydrogel-based encapsulation has also been used to create simple protocell models using scalable multicompartment DIB systems. These models may be scaled up to eventually create proto-tissues and proto-organs [76]. Also, encapsulating DIBs in hydrogel chassis using microfluidic chip to create "eDIBs" has proven to improve the handling as well as the applicability of DIBs outside the lab environment [77].

2.3. Encapsulating networks of DIBs in a thermosensitive organogel

Continuing along this path, we present the fabrication of a liquid-in-gel membrane-based material based on the encapsulation of networks of DIBs. It is inspired by the work done by Venkatesan *et al.*, albeit with additional improvements and optimization of the SEBS-hexadecane organogel with the vision of creating a self-supporting and stimuli-responsive material composite inspired from cell membranes. The following sections discuss the concept behind the creation of membrane-based materials as well the manufacturing steps towards the creation of the liquid-in-gel functional material composite.

2.3.1. Concept

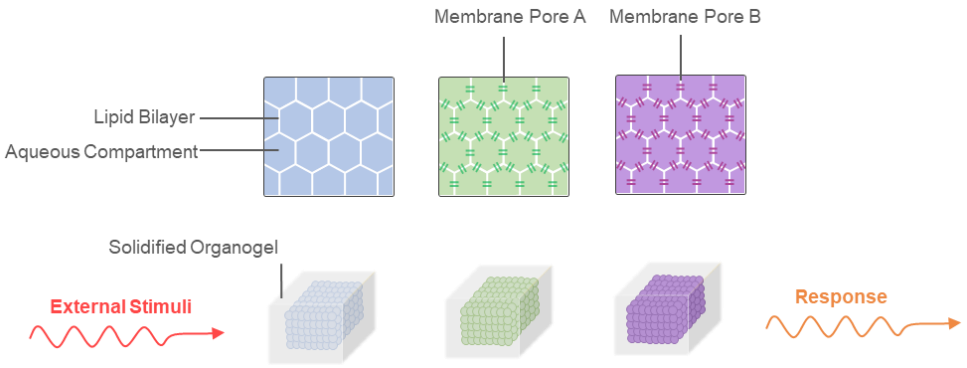

Figure 15 - Self-supporting stimuli-responsive biomolecular material. Networks of DIBS may be encapsulated in a self-supporting organogel. The resulting material could be functionalized with various membrane proteins and peptides to achieve different responses.

Similar to tissues, multiple DIBs may be organized into large interconnected droplets assemblies with specific and various functionalities [59, 63, 78] (Figure 15). Through encapsulation with SEBS-Hexadecane, the functionality of assembled droplets combined with the mechanical properties of the organogel gives rise to synergistic attributes [68]. One key advantage of SEBS-hexadecane organogel is its ability to liquify at higher temperatures while being a solid-like structure at room temperature. However, the threshold temperature upon which the liquid/solid transition occur is highly dependent to the polymer-to-oil ratio. Therefore, the concentration of the organogel is optimized while taking into consideration the organogel's compatibility with DIBs at higher temperatures while remaining self-supporting at room temperature. In addition, when compared to other polymers, the SEBS polymer offers higher stability and robustness against degradation [79, 80].

Here, DIB networks are constructed using the droplet printer discussed in the previous sections. In this section we introduce membrane proteins and peptides in the droplets and we show that the pores remain functional within the membranes after the heating and cooling cycles. We

also demonstrate that not only does the SEBS preserve the structural integrity of the DIB network, but it may also add to their functionality. Self-supporting gels may act as a physical buffer between the network and the outside world by channeling controlled external mechanical stimuli to regulate the size of the membranes similar to the regulated attachment method (RAM) for single DIBs. [81]

2.3.2. Design space and viscoelastic properties of the organogel

The viscoelastic properties of the organogel are tuned to have favorable properties at high and low temperatures, allowing for printing at elevated temperatures then sealing the droplets at typical working conditions. Here, this is done by analyzing the rheological results of various polymer-to-oil ratios. Previous studies investigated the usage of a 10 mg/mL of SEBS in hexadecane concentration to improve the portability and durability of DIBs. At this concentration, this organogel is a viscous gel that provides some protection but is not self-supporting at room temperature.

A straightforward solution to this challenge would be to increase the polymer content inside the organogel to improve its stiffness at room temperature. However, higher concentrations of SEBS in the organogel results in a higher melting point. Recall that the organogel must be in the liquid form (i.e. at higher temperatures) to print DIBs. Biological components in DIBs especially membrane proteins are prone to thermal degradation beyond a temperature of 65°C [17, 82-84]. This limits the working temperature to be $\leq 60°C$ and with it the polymer-to-oil ratio. For these reasons, it important to find the optimized design space for the organogel.

Rheological studies for increasing concentrations of SEBS in hexadecane by 10 mg/ml reveal an increase in both storage and loss moduli by a little less than an order of magnitude (Figure 16). Physically, this could be explained by the decreasing separation of the copolymer micelles

coupled with decreasing expansion of the midblock bridges as the concentration of the polymer increase.

Alternatively, elevating the temperature of the organogel makes it to lose its elasticity and becomes gradually viscous. At a temperature T_{co}, the modulus of elasticity *G'* cross-over the loss modulus *G"* before asymptotically approaching a plateau (Figure 16). At this point, the organogel behaves more like a viscous liquid than a solid, as the loss modulus *G"* is dominant. We noticed that an increase in the polymeric concentration in the organogel, shifts the cross-over temperature T_{co} into higher values. However, for a specific concentration of polymer, at a temperature $T > T_{co}$ + 25 °C, convective currents are observed in the organogel phase due to the Marangoni effect. We experimentally found that the ideal temperature range lies between $T > T_{co}$ + 15 °C and $T > T_{co}$ + 25 °C for a given organogel concentration. In this range, the organogel is viscous and stable enough for droplet printing.

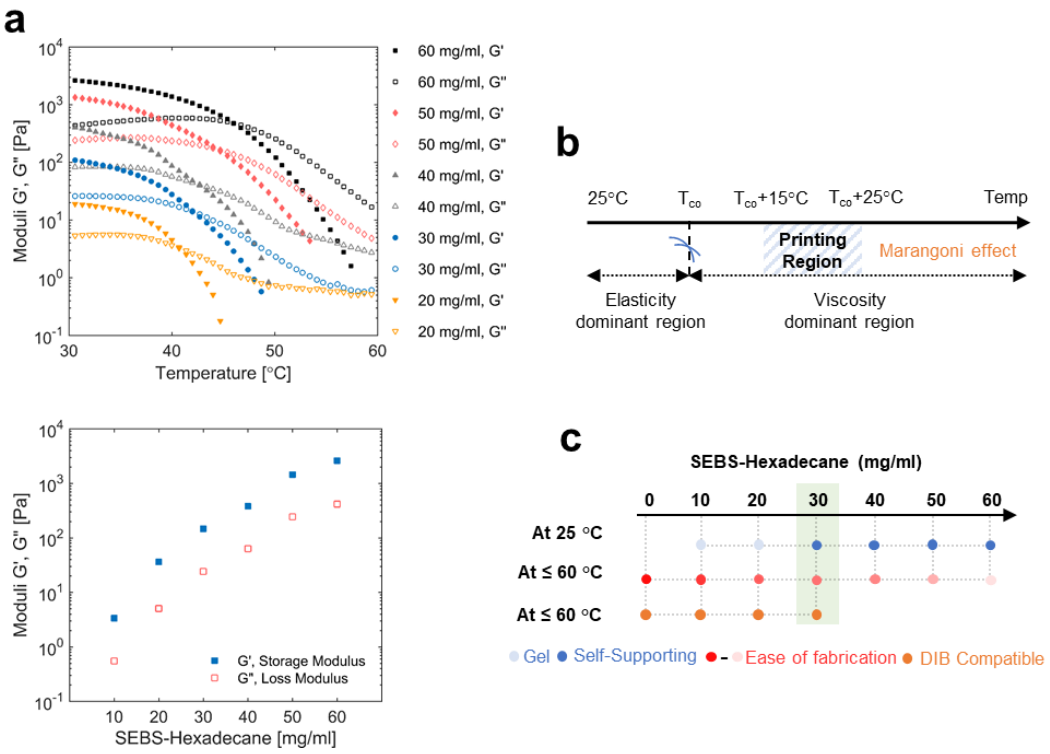

Figure 16 - a) Viscoelastic characteristics of different SEBS-Hexadecane concentrations, from [68]. The T_{co} which corresponds to the temperature at which both moduli cross-over increase with the increasing concentration of SEBS in hexadecane. At room temperature, both loss and elastic moduli increase by almost an order of magnitude with every increase of 10mg/mL in the organogel concentration b) The printing range is empirically found to be between 15°C to 25°C above T_{co}. Below that it is too viscous to form DIBs and beyond that range, Marangoni effects are observed c) The optimized organogel concentration with favorable viscoelastic properties is found to be 30mg/ml.

Combining the above constraints, we found that a concentration of 30 mg/ml is the ideal SEBS-to-Hexadecane concentration (Figure 16.c). At this concentration, the organogel is self-supporting meaning it is capable of supporting its own weight – a characteristic not found in lower concentrations – and it is soft elastic solid with an elastic modulus of 120 similar to the brain and central nervous system. Plus, its printing temperature range is less than 65 °C, which makes it compatible with reconstituting membrane proteins and peptides in large networks of DIBS of consistent droplet size without the risk of thermal degradation.

Next, we assessed how would a concentration of 30 mg/ml affect the membrane properties at high (i.e. 60 °C) and at room temperature. We compared the specific capacitance measurement from literature and a control experiment using the Gross *et al.* [57] approach and compared it to the one obtained with 30 mg/ml. The measured values of specific capacitance at SEBS in oil at high and low temperatures were comparable to those found in the control experiments (Table 1).

Table 1 - Specific Capacitance at room and high temperature

Solvent	**Specific Capacitance ($\mu F/cm^2$)**
Hexadecane (RT)	0.751 (±0.06)
Hexadecane (60°C)	0.534 (±0.03)
30mg.ml^{-1} SEBS-Hexadecane (RT)	0.713 (±0.07)
30mg.ml^{-1} SEBS-Hexadecane (60°C)	0.609 (±0.13)

Therefore, a 30 mg/ml is chosen to be the concentration for the creation of the stimuli-responsive material because it has favorable viscoelastic features at room temperature and at ≤ 60 °C while having minimal effect on the membrane properties. This allows for the creation of self-supporting organogels fully encapsulating and insulating the printed DIB networks as shown in Figure 17.

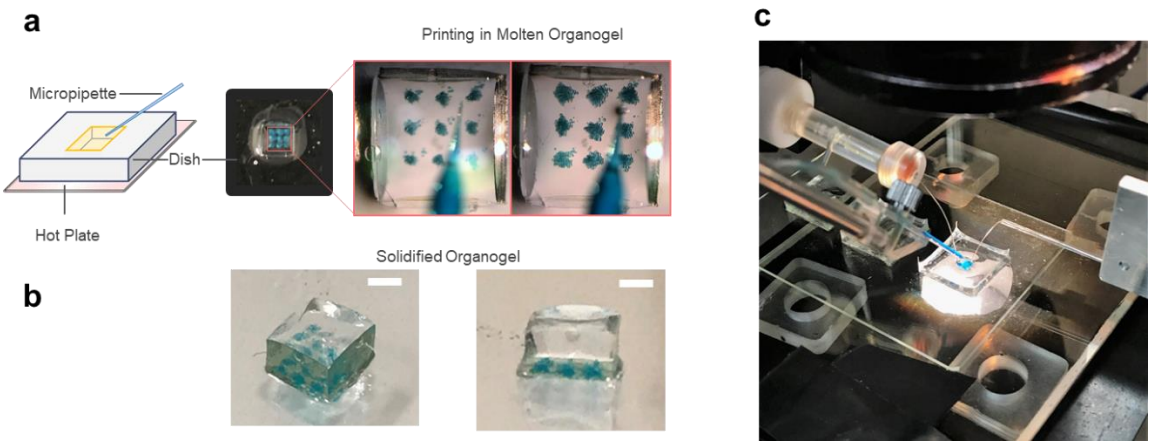

Figure 17 - Printing and encapsulation of 3x3 “mounds” of droplets before encapsulation at room temperature. The resulting composite is self-supporting as it is scooped out of the dish.

2.3.3. Printing and encapsulating large networks of DIBs

Formation of large network of DIBs does not affect the fundamental electrical properties of its constitutive membranes. In that sense, the electrical model discussed in section 1.6, still stands in the individual membranes. Scaling up the electrical model of a single membrane, networks of DIBs may be approximated as a large circuit of RC circuits connected in unsystematic configurations.

To assess the electrical properties of encapsulated DIBs in a 30 mg/ml SEBS-hexadecane concentration, we printed large networks of droplets (>2000 droplets). Two large droplets were first manually formed at the tip of two agarose coated Ag/AgCl electrodes before printing the smaller droplets around them. Once a connected path of droplets was formed between the electrodes – which is equivalent to a closed electrical circuit – a gradual and continuous increase in the capacitance was observed before reaching a plateau at 3.2 nF (Figure 18.b).

After printing, the organogel is left to cool down to room temperature, during which it solidifies and encapsulates the droplets without affecting their geometry. Upon cooling, the overall

capacitance measured across the membranes rose to 4 nF, which could be explained by the continuous thinning of the membranes (i.e. expulsion of the oil from the membranes) due to the decrease in temperature.

The organogel-droplets composite was left at room temperature for 20h. Some but not all of the bilayers remained stable across the electrodes which may be inferred by the decrease in the network's capacitance to 1.2 nF. This could be explained though by the coalescence of certain bilayers or the evaporation of some of the droplets – phenomena previously observed in DIB networks [85].

When reheated, the organogel liquifies. Electrical investigation of the network during reheating revealed an increase in the overall capacitance to around 3 nF (Figure 18.c). This could be attributed to the formation of new bilayers between the droplets as the surrounding solid matrix relaxes and loses its elasticity [68].

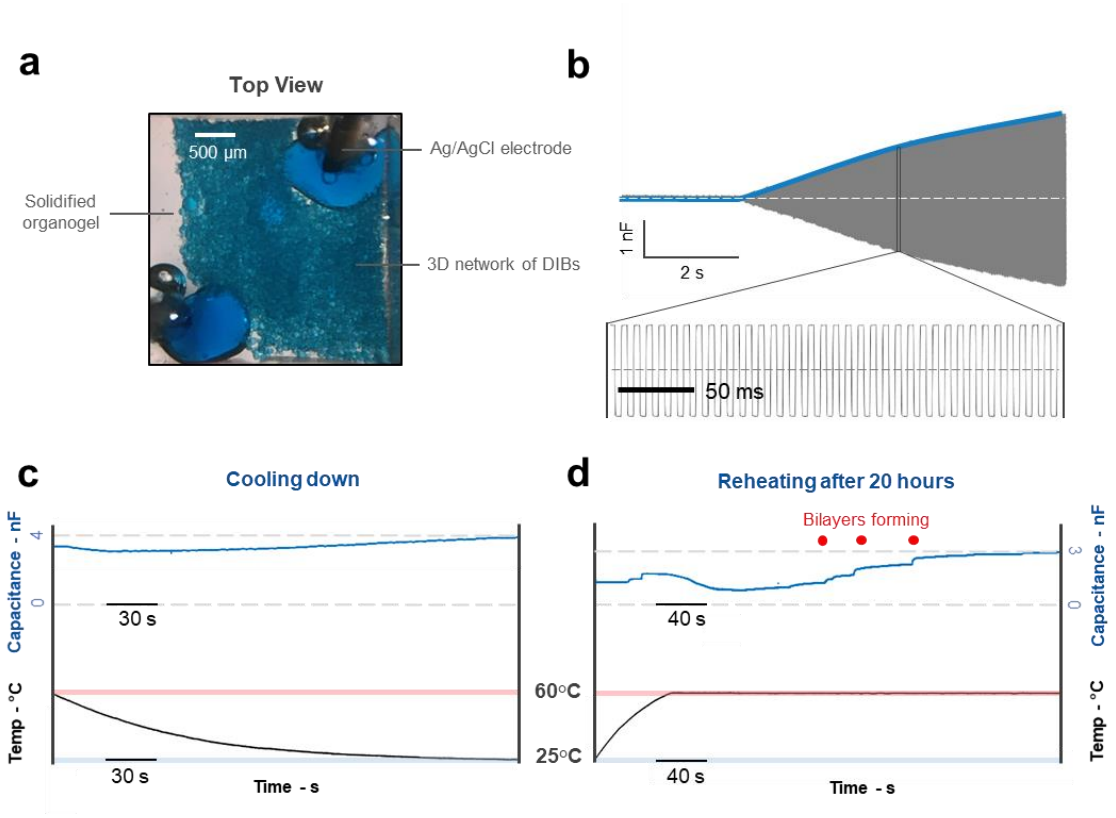

Figure 18 - a) Printing large networks of DIBs in 30 mg/ml SEBS-Hexadecane at 60°C b) Continuous increase in the capacitance once a pathway of connected droplets is established between the electrodes c) At it cools down, the organogel encapsulates the droplets. The resulting capacitance is observed to slightly increase, likely due to the continuous exclusion of oil from the membranes d) When heated again after 20h, the capacitance increases in a step-wise fashion likely due to the reformation of some bilayers between adjacent droplets.

2.3.4. Biomolecular functionality of encapsulated membranes

Now that the encapsulation of the droplets in a SEBS proved to have little effect on the capacitance measurements, the next step would be the reconstitution of proteins and peptides in the encapsulated membranes that will give them stimuli-responsive functionalities.

Here, we especially targeted the incorporation of αHL pores and voltage-responsive peptides Alamethicin, which are typically used in DIB systems. Their activity is probed at room conditions whereby the organogel is in its solid form. We first investigated the activity of αHL in a single membrane encapsulated in 30mg/ml SEBS-Hexadecane (Figure 19.a) before printing a

large network of DIBs containing αHL pores. Once a bilayer forms between adjacent droplets, the monomers spontaneously insert into the bilayer and create a conductive pore. Such pores allow the transport of ions between adjacent droplets rendering the membranes rather permeable. From an electrical standpoint, this could be seen as a stepwise increase in the conductance of singular bilayers in response to a DC voltage where each step corresponds to an individual insertion of a pore. The conductance of these pores was found to be 0.38 ± 0.05 nS (n = 5) in a bilayer formed at at 60 °C and then brought to room temperature which is comparable to the activity of αHL in hexadecane only (0.36 ± 0.06 nS, n = 5). However, in a large collection of droplets (in this case, > 2000 droplets, Figure 19.b), these steps become less and less pronounced as the network grows larger. At this point, individual insertions do not affect the total contributions of the pores in the DIB networks. Eventually, applying a DC voltage across the network will result in a flat line current response related to its overall conductance.

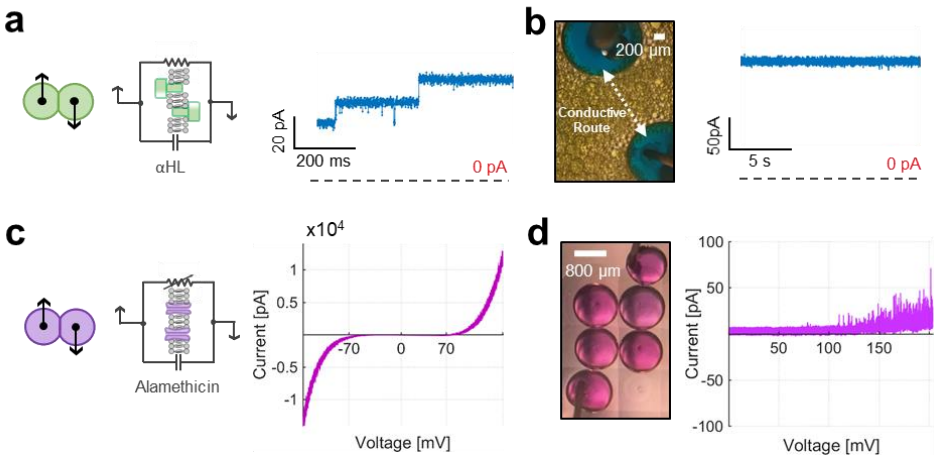

Figure 19 - Biomolecular functionality. a) αHL pores incorporated in a single encapsulated membrane shows the typical discrete increase in the resistive current response across the membrane with respect to an applied DC voltage b) in large networks containing αHL (yellow), however, the overall resistive current across the membrane is a function of all the membranes containing αHL . In this case, applying a DC voltage results in a constant current response as individual pore insertion become less pronounced c) Voltage-sensitive peptide Alamethicin (Alm) incorporated in a single membrane also show the same gating threshold of around 70 mV in a Cyclic Voltammetry experiment d) In large networks, applied voltage is divided across the membranes. In this case, the voltage threshold of the overall system is shifted to a higher value.

Next, we repeated the same experiment with alamathecin peptides which provides a voltage-dependent conductivity. We compared the activity of alamethicin peptides in membranes surrounded by the organogel and by hexadecane alone. The results have shown minimal difference in both behavior as alamethicin peptides gated exclusively above a voltage threshold of around 70 mV [68, 86-88] (Figure 19.c). Furthermore, the probability of gating increases with the rise in membrane potential through cyclic voltammetry. This gating likelihood is manifested as a non-linear voltage-current behavior resembling that of a diode or a voltage-dependent resistor.

The behavior of alamethicin becomes harder to investigate in networks of DIBs. While the same nonlinear behavior stands, the gating threshold shifts, and gating happens at a higher voltage potential across the network. This is mainly because the applied voltage is distributed among the droplets [89], causing the gating likelihood to decrease as well for a given voltage. The shift in the gating threshold was further corroborated when a CV was applied across 2-by-2 network of DIBs (Figure 19.d).

Due to the minimal changes in the behaviors of both αHL and alamethicin channels in regular liquid-in-liquid setups and liquid-in-solid setups, the encapsulated membranes may remain functioning. This also confirms that the bilayers formed in the organogel are indeed lipid-based and not polymeric-based.

2.3.5. Mechanical functionality of encapsulated membranes

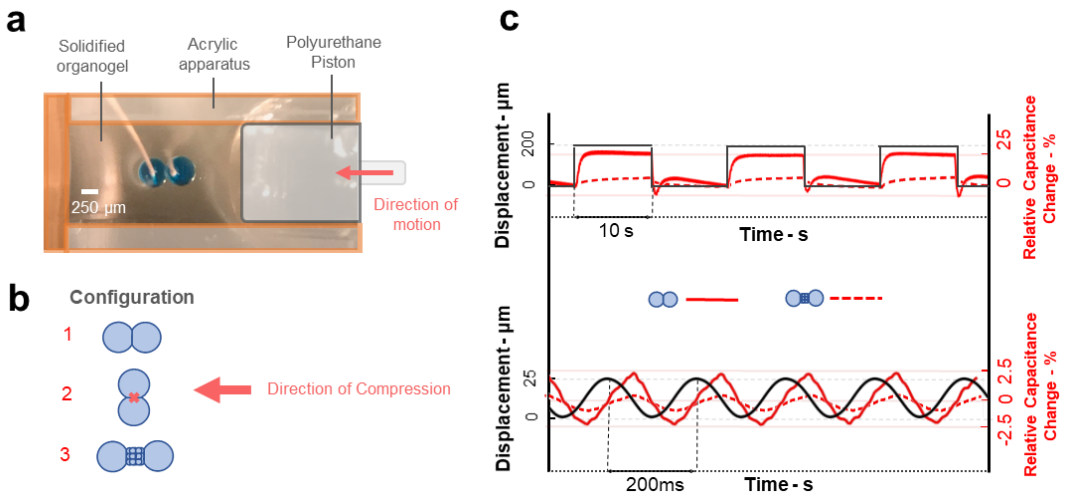

Figure 20 - Mechanical Perturbation of encapsulated DIBs a) a polyurethane piston is used to apply mechanical compression on encapsulated DIBs b) different configurations of DIBs are used where either the directionality of the force with respect to the membrane is changed or the number of bilayers is changed c) changes in the capacitance (due to change in the membrane(s) area) after the application of a rectangular and a sinusoidal displacements were observed only in configurations 1 and 3. In case 2, the bilayer would rupture under mechanical perturbation.

In the most liquid-in-liquid DIB approaches, the lipid bilayer may expand and contract due to applied external mechanical force before it reaches an equilibrium [18]. In the encapsulated membranes case, the mechanical perturbation is directly applied to the organogel. The droplets in turn deform, channeling the mechanical deformation into the changes in the membrane dimensions.

By encapsulating the membranes, the organogel acts as a viscoelastic buffer between the external environment and the DIBs. Furthermore, the bilayers dimensions may be regulated by applying mechanical forces to the solid organogel. This was demonstrated using a piezoelectric transducer to apply cyclical deformation to the organogel-droplets composite while examining the changes in the capacitance. These capacitive changes would reflect the overall variations in the bilayers due to the applied mechanical forces (Figure 20).

Three different DIB configurations were examined: two cases were done using a single membrane to test the effect of directionality between the force applied and the membrane, and one case that included the application of mechanical force to a collection of small droplets. The mechanical vibrations were applied systematically in a step (5 mHz, 200 μm) or in a sinusoidal displacement (5 Hz, 25 μm).

In the cases that involve a singular membrane, changes were only observed when the applied force was perpendicular to the membranes while, in the other case, the single membrane either slightly varied or ruptured. Step displacement with an amplitude of 200 μm applied to the first case, showed a maximum increase of 25% in the capacitive current (almost 20 μm in bilayer diameter). When the compression is ceased and the organogel is released back to its original position, the capacitive responsive decreases instantaneously, and overshoots below the original capacitance before going back to its initial and equilibrium value. Alternatively, once a sinusoidal wave is applied, an out-of-phase alternating current response followed with changes up to 2% and a lag of $\frac{\pi}{4}$ rad. This lagging behavior may be attributed to the viscoelastic nature of the organogel.

On the other hand, compressing a 3D network of droplets revealed the same trends albeit with lower changes in the capacitance. This could be explained by the relatively smaller size of the intermediate droplets (~100 μm compared to ~700 μm in the single membrane cases). Smaller droplets tend to yield smaller bilayer interfaces as well as an increase in the stiffness of the surrounding organogel [90-92].

The ability to regulate the size of a lipid bilayer through encapsulation gives rise to potential applications in sensing and actuation. In this sense, encapsulation does not only help preserving the structural integrity of DIBs and improve their robustness, but it could also give

additional functionalities that are not normally found in fluidic DIBs. For instance, by incorporating membrane proteins such as MscL in the bilayer, the material may be used as a biomolecular strain gauge.

2.4. Discussion and Summary of Chapter 2

This chapter discusses the creation and functionalization of large 3D networks of DIBs. A novel pneumatic-based droplet printer is presented and is used to print 2D and 3D structures of DIBs in oil and in molten organogel. To improve the durability and portability of these networks, we encapsulated the DIB network in a thermosensitive organogel that consists of SEBS triblock copolymer mixed with the hexadecane oil. The organogel is optimized with constraints related to obtaining suitable conditions for printing droplets with biomolecular components and self-supporting capabilities at room temperature.

CHAPTER 3

MICRO-MEMBRANE HYDROGEL ELECTRODES

3.1. Concept

The following chapter will examine the usage of the self-assembly of lipid bilayers to create a hydrogel-based membrane electrode inspired by DIBs and DHBs. The novel electrode will allow for noninvasive rapid screening and studies of lipid bilayers. DIBs and DHBs have emerged as powerful tools for screening droplet contents due to their relatively ease of fabrication and their ability to form, separate and then reform lipid bilayer. This has been employed to screen and study membrane proteins and transport phenomena across lipid membranes.

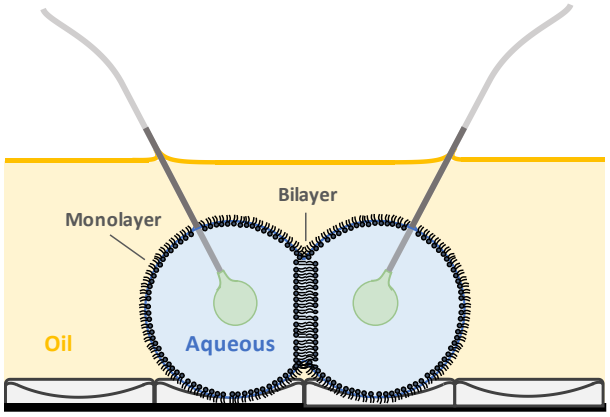

Figure 21 - Droplet interface bilayer suspended from silver/silver chloride electrodes

However, membranes created using these methods are relatively large and are on the order of hundreds of microns in diameter. Comparatively, these membranes are much larger than those found in cell membranes. Furthermore, such bilayers are fundamentally metastable, take a

relatively long time to form depending on the droplet size and the selected solvent, and often times may rupture due to droplet coalescence or fusion.

Here, we address these drawbacks by developing a new electrode using a hydrogel-supported lipid monolayer. The novel electrode is based on the extrusion of a small hydrogel patch from the tip of a pre-pulled insulating glass capillary. This capillary contains the rest of the hydrogel solution which is surrounding a silver/silver chloride Ag/AgCl electrodes.

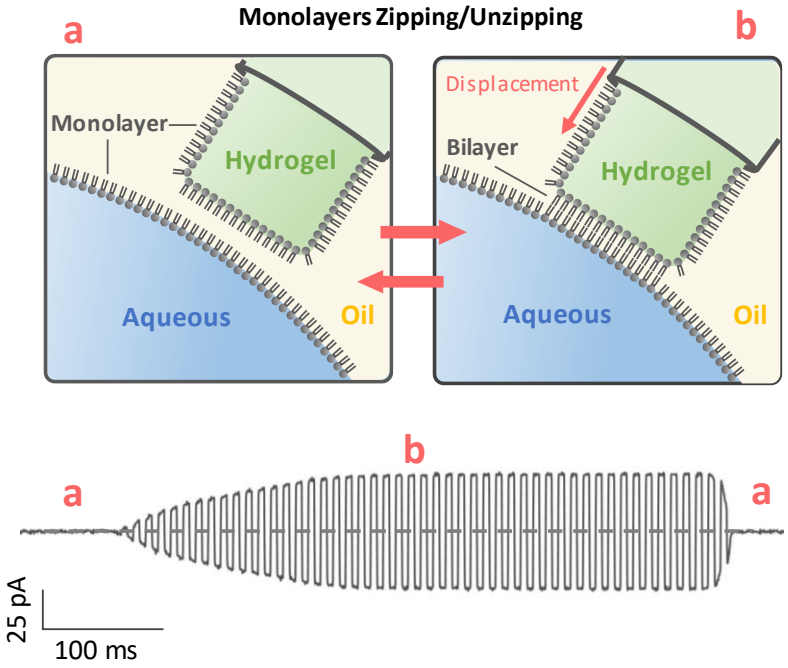

Figure 22 - Micromembrane electrodes. Formation and separation of the micromembranes by displacement of the MMHE

The resulting micromembrane hydrogel electrode, or MMHE, may be implemented in applications for quantifying membrane properties and studying membrane-active species. One key advantage offered by MMHEs over other hydrogel supported lipid membranes is their ability to form, separate and then reform a lipid bilayer on demand by simple displacement (Figure 22).

Subsequent formation of lipid bilayer happens with minimum contamination, making it a good candidate for the screening of large arrays of droplets.

3.2. Fabrication

The micro-membrane electrode consists of a pulled glass micropipette filled with a UV cured PEG-DMA hydrogel surrounding a silver/silver-chloride (Ag/AgCl) electrode embedded inside the micropipette (Figure 23). Several heat-pull protocols are developed for the micropipette puller (P-1000 Sutter instruments) to consistently fabricate short-taper shaped glass micropipettes with inner diameters ranging from 10 µm to 30 µm from an initially flat tip borosilicate glass micropipette (OD 1 mm, ID 0.5 mm).

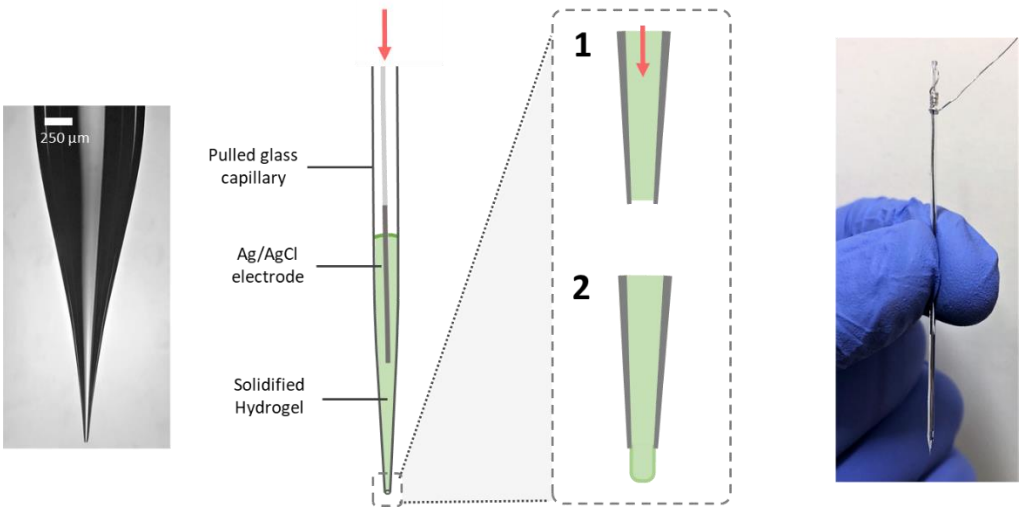

Figure 23 - Fabrication of the MMHE. a) Short-tapered pipettes are used to prepare the MMHE b) Once the photopolymerization step is completed, a little pressure is applied to the Ag/AgCl electrode to extrude a small patch of hydrogel outside the tip of the capillary.

Using a MicroFil (World precision instruments, 34 gauge, 67mm long), the fabricated glass micropipette is filled with the hydrogel solution. Once exposed to UV light (3 minutes, 1 W intensity, 365 nm source), the hydrogel undergoes free-radical photopolymerization. During this

process, crosslinked polymeric structures are induced [93, 94] and the hydrogel gradually stiffens around the wire electrode. The water-swollen hydrogel not only helps conducting the ionic current measured at the membrane level but also fastens the electrode within the capillary.

After the curing step, the solidified hydrogel remains trapped inside the micropipette within few microns away from the tip (Figure 23). This is undesirable as it impedes the cured hydrogel from reaching the aqueous phase in oil to form a lipid bilayer and results in a layer of trapped insulating oil within the MMHE as it is immersed. For this reason, the wire electrode is manually pushed inside the micropipette to force the surrounding hydrogel to be extruded into a miniature cylindrical-like patch outside the tip of the capillary (Figure 23). The diameter of the exposed hydrogel corresponds to the inner-diameter of the pulled glass capillary with a height typically ranging from 10 to 40 μm.

On the other end of the glass capillary, the extended silver wire is carefully twisted around the micropipette to further secure the hydrogel-electrode assembly. Because water-swollen hydrogels are prone to dehydration in air, the tip of the electrode is quickly submerged in the oil phase. A crocodile clip is used to attach the coiled wire to the ground.

3.3. Mechanics of Membrane formation

Lipids molecules may be dissolved in either the oil or aqueous phases. Owing to their amphiphilic nature, the lipids would spontaneously self-assemble at the oil-aqueous interface and the oil-hydrogel interface. Here, lipid bilayers were formed between the MMHE and the aqueous interface was only achieved when lipids were introduced in the oil phase (Lipids-Out), in both the aqueous and the hydrogel phases (Lipids-In) or in all phases. DPhPC (1,2-diphytanoyl-*sn*-glycero-3-phosphocholine) lipids were used to form the bilayers in most of the experiments because they are previously extensively studied, form relatively stable membranes, and do not undergo phase

transition under the presented working conditions. However, this method also permits the formation bilayers using other naturally occurring and unsaturated lipids molecules such as DOPC (1,2-Dioleoyl-*sn*-glycero-3-phosphocholine) when introduced in the oil phase which is proven to be challenging using other methods such as DIBs [95]. After its fabrication, the MMHE could be mounted on a piezoelectric actuator and centered above an inverted microscope (Leica DMI3000B). This gives the advantage of automatically creating and unzipping the bilayer without breaking it by simply displacing the electrode using the piezoelectric actuator. It also allows the application systematic mechanical vibrations during electrophysiological studies of the membrane. Once the MMHE is brought into contact with the aqueous phase both monolayers zip into a lipid bilayer.

One advantage offered by this method is the ability to regulate the membrane size mechanically by inserting the electrode into the aqueous phase. This causes the elastic membrane of the aqueous phase to bend and wrap around the MMHE. Consequently, the bilayer is observed to grow hydrogel is engulfed within the droplet. This additional growth in bilayer area is reflected by the continuous rise in the capacitance from an initial value C_0 of 6 pF following the displacement of the MMHE. The capacitance eventually reaches a maximum steady-state value C_{max} of 18 pF. Interestingly, beyond this point, additional displacement of the electrode within the aqueous phase does not increase the capacitive current. Also, it neither ruptures the membrane nor drastically change the resistance across the membrane. Also, this indicates that the maximum bilayer area offered by the hydrogel is reached (Figure 24.b).

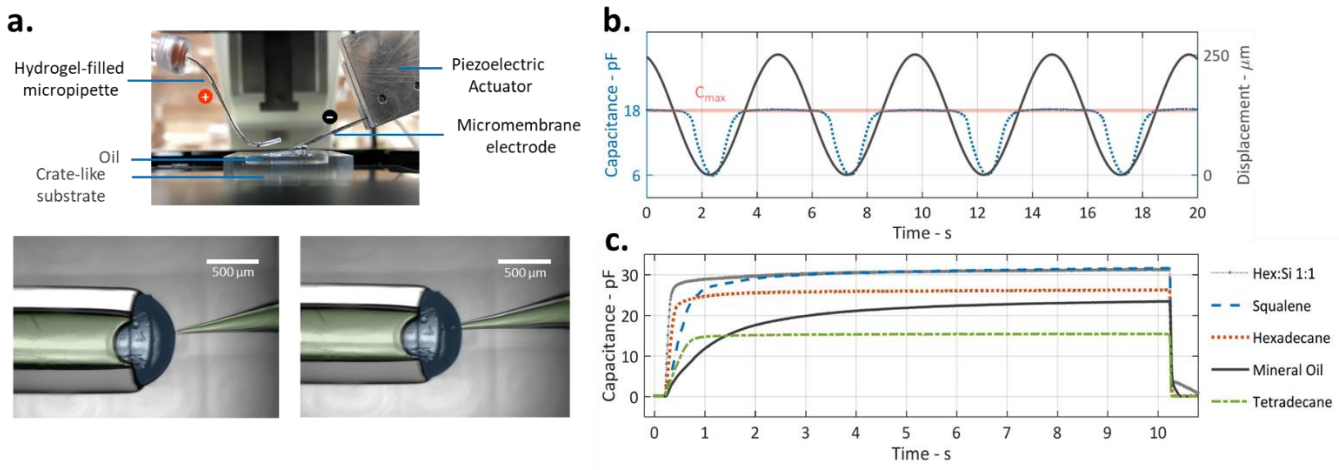

Figure 24 - a) The MMHE may be mounted on a piezoelectric actuator that controls its displacement. The membrane is formed once the MMHE is pushed toward the aqueous surface b) applying displacement to formed membranes shows an increase in capacitance with a maximum C_{max} value that is related to the geometry of the hydrogel patch and the mixtures used. c) A lipid bilayer may be formed using MMHE in different oils that are typically used in DIB studies.

The maximum bilayer area could be calculated to be ~3400 µm^2 using C_{max} and the specific capacitance of the bilayer (Hex:Si AR 20 1:1, 0.5 mg.ml^{-1}, DPhPC lipids out). Assuming that the extruded hydrogel is geometrically similar to a bottomless cylinder with a 30 µm diameter, the height of the cylindrical hydrogel could be calculated to be ~28 µm which is similar to the one visually measured.

Next, we demonstrated that the MMHE could be used to form membranes in different oils (Figure 24.c). During these experiments, the same microelectrode is used while changing different dishes containing various oil-lipid mixtures. The result showcase that for the quasi-consistent geometry of both the hydrogel and the supported aqueous drop in each experiment, lipid bilayers take few milliseconds to ≥10 seconds to form depending on the oil type. The variations in bilayer formation times are largely due to the combining effects of the energy of adhesion of the monolayers and the viscosity imposed by the different surrounding oils.

3.4. Reconstitution of membrane proteins and peptides

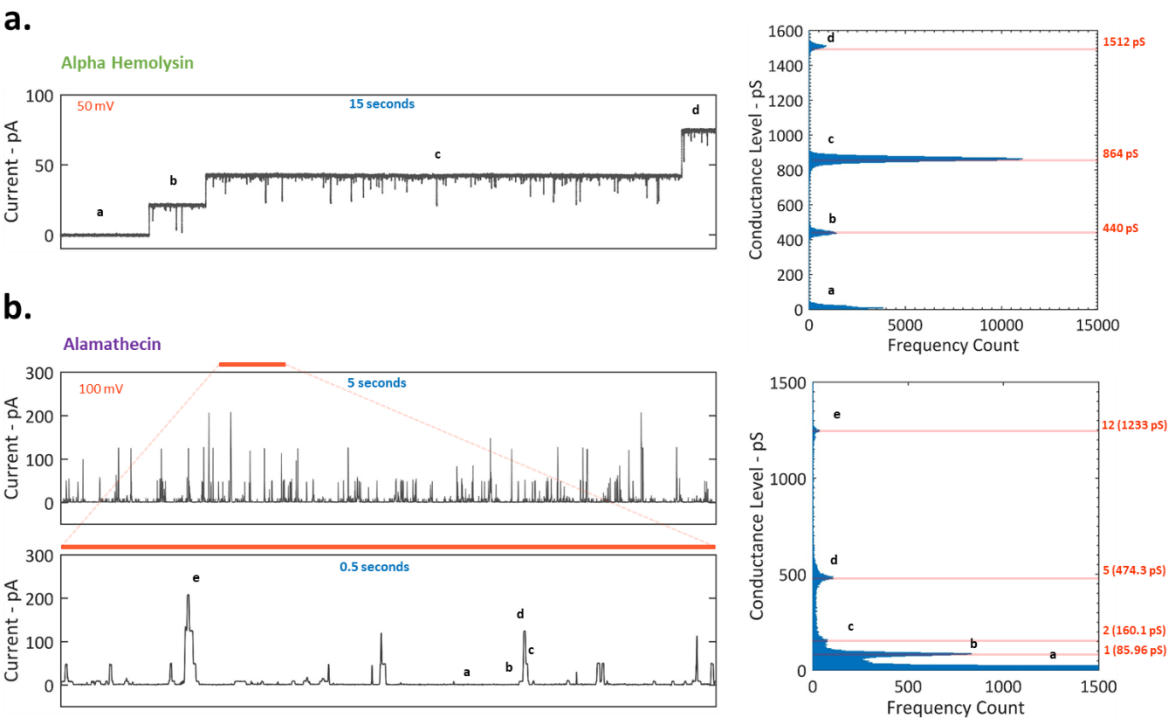

Figure 25 - Alpha-hemolysin and alamethicin in MMHEs a) αHL pores may be incorporated and reconstituted in MMHE-based membranes showing a high-degree of precision with comparable conductance values to those shown in regular DIB studies b) alamethicin peptides show the same stochastic behavior of gating "spikes" after the application of 100 mV DC voltage. The conductance levels of the alamethicin are easy to discern.

Next, we probe the activity of membrane proteins and peptides to further confirm the formation of a lipid membrane at the hydrogel surface. We reconstituted alpha hemolysin (αHL) and alamethicin (alm) because of their common usage in DIB studies as discussed in the previous chapter. This offers an adequate point of comparison for membrane channels activities with previous studies done with DIBs.

Shortly after the bilayer formed between the MMHE and the aqueous phase containing αHL, the pores began forming within the membrane (Figure 25.a). This was observed as a stepwise increase after the application of the transmembrane DC potential of 50 mV. The discrete changes

in the conductivity of the membranes due to αHL insertion are in line with those found in the literature [68, 96]. Once the MMHE is retracted from the aqueous phase, the membrane separates and disconnects all the pores already formed. Reinsertion of the electrode restarts this process.

Alternatively, another aqueous solution containing a mixture of alamethicin peptides with liposomes was used. After bilayer formation between the MMHE and the aqueous droplet, alamathecin peptides partially insert in the membrane. A constant transmembrane potential of 100 mV is applied to induce gating events. The result is sequence of discrete stepwise “spikes”, where each step corresponds to a conductance level (Figure 25.b). Both tests demonstrate the formation of a functional membrane at the surface of the MMHE.

3.5. Cyclic formation and separation lipid bilayers

To evaluate the robustness of MMHE, we investigated the repeated formation and separation of bilayers. This was done by applying a square wave displacement to the piezoelectric actuator holding the electrode. As a result, the tip of the electrode alternates between outside the droplet or fully immersed in the aqueous phase at a 1 Hz frequency. During this process the capacitive current response was monitored by sending a 100 Hz, 10 mV peak to peak triangular wave to the bilayer (Equation 1). The changes in the capacitive current reflect the dynamic variations in the membrane size due to the movement of the electrode.

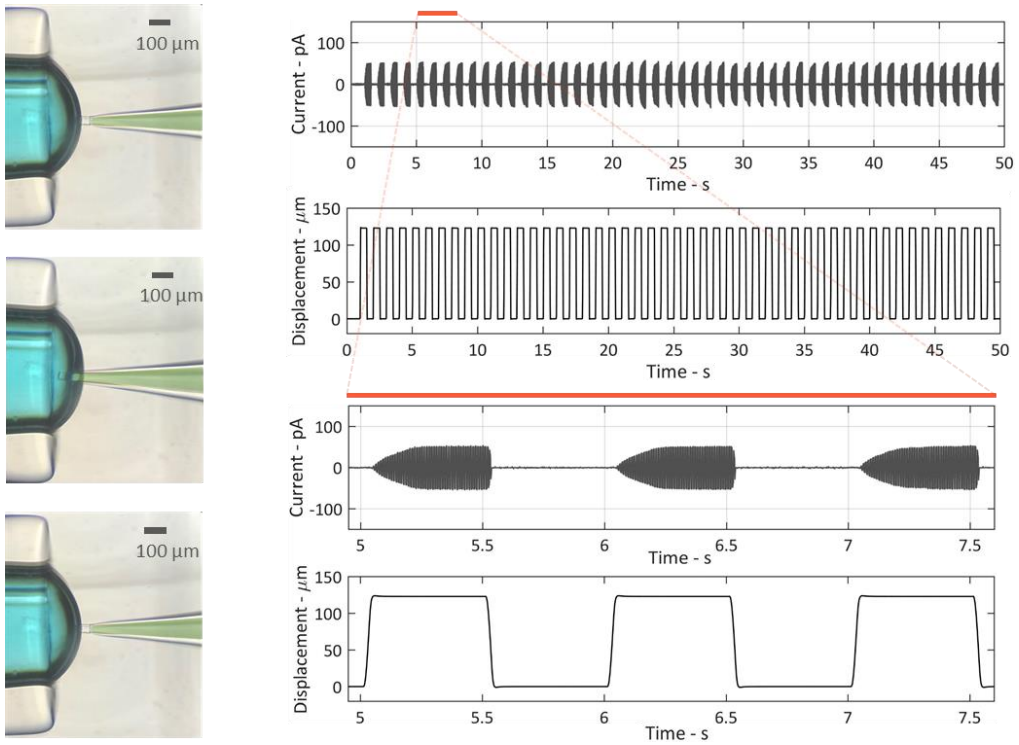

Figure 26 - Forming and separating bilayers may be achieved using MMHE in a cyclical fashion without rupturing or damaging to membranes. This paves the way towards fast membranes screening and detection studies using MMHEs.

Each time the electrodes were inserted in the aqueous phase, the bilayer rapidly grew before reaching a maximum value as discussed in section 3.3. Moreover, the maximum capacitance was highly consistent across all the cycles. When the electrode separates from the aqueous phase, the membrane instantly separates, and the capacitance goes back to zero. This process was consistent and highly repeatable for several hundreds of cycles without rupturing the bilayer. On a side note, the formation of the bilayer was not contingent upon the precise placement of the electrode relative to the aqueous phase. In fact, the MMHE could be placed at various angle relative to the surface of the aqueous phase.

3.6. Asymmetric membranes

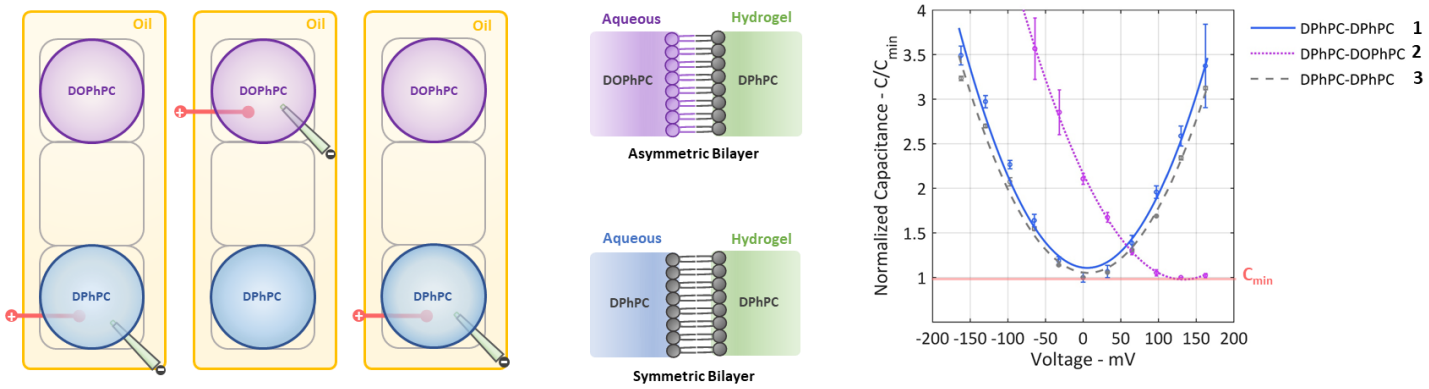

Figure 27 - Asymmetric membranes may be formed using MMHE by dissolving various types of lipid in the aqueous and hydrogel phases. For instance, DPhPC/DPhPC and DOPhPC/DPhPC membranes may be formed sequentially without the risk of contamination. This is supported by finding the minimum capacitance values while changing the voltage across the membranes.

As previously shown in section 3.3, MMHEs possess a maximum capacitance value related to the geometry of the extruded area as well the properties of selected the lipids and oil. Therefore, other methods may be used to probe the bilayer such as electrocompression and membrane thinning [57].

Rather than mixing the lipids with the oil phase, they may be introduced in the aqueous phases. This allows the creation of localized monolayers in the oil phase where the lipid would remain in the aqueous phases without diffusion into the lipid-free oil. Here, DPhPC lipids were introduced in the hydrogel phase of the MMHE. The electrode was subsequently used to pierce two aqueous droplets, one containing DPhPC and the other containing the ether lipid 1,2-di-O-phytanyl-sn-glycero-3-phosphocholine (DOPhPC). By puncturing each of the droplets, the MMHE containing the DPhPC lipids is able to create symmetric DPhPC/DPhPC bilayers and asymmetric DOPhPC/DPhOPC bilayers. These asymmetric membranes possess varying dipole potentials due to the difference in their linking groups.

A stepwise transmembrane voltage was applied to the formed membranes ranging from -162.5 mV to 162.5 mV with step a size of 32.5 mV. At every step, the equilibrium membrane capacitance was measured. The plot of the capacitance values may be approximated by a 2^{nd} order polynomial plot. Physically, the minimum capacitance is attained when the electrostatic asymmetry of the membrane is balanced by the values at the boundary [97]. In the case of a symmetric bilayer, such as the DPhPC-DPhPC membrane, the minimum capacitance is at 0 mV whereas with asymmetric membranes such as the DOPhPC-DPhPC membranes it corresponds at 135 mV (Figure 27), matching the expected difference in electrostatic potential profiles [18, 98].

Moving the MMHE between the droplets and separating/reforming the membrane produces no changes in the recordings. This may be explained by the fact the lipid bilayer unzips when the MMHE is displaced away from the droplet interior. Therefore, the changes in the composition of a leaflet is negligible due to the relatively smaller bilayer area and the slow lipid flip-flop rate. This could be tested by using the same MMHE to create a symmetrical and then an asymmetrical membrane sequentially while performing the same capacitance vs potential measurements at every step. Results revealed no shift in the electrostatic offset (Figure 27) confirming that MMHEs may be employed for screening the composition of many different droplets.

CHAPTER 4

CONCLUSIONS

The self-assembly of amphiphiles such as lipids and proteins is used to develop and advance the field of model membranes. By approximating the structure and functions of cells, model membranes are able to replicate complex physiological phenomena that take place at the surface of cells. Recently, droplets interface bilayers (DIBs) have been presented as a powerful tool to study such phenomena, due to its ease of fabrication, robustness and ability to faithfully reconstitute stimuli-responsive membrane proteins and peptides. In this model, two fluidic aqueous droplet acts as a support for the lipids bilayer that form at their plane of intersection. Moreover, DIBs are scalable and capable of forming large networks of membranes with additional emerging functionalities.

The functionalities found in lipid models in general and in DIBs in particular, are harnessed here, to develop 1) novel stimuli-responsive biomolecular materials and 2) micromembrane hydrogel electrodes (MMHE). The biomolecular material relies on the creation of large networks of DIBs with functional properties. To this end, an automated pneumatic-based droplet printer is developed to print large network of DIBs with specific architectures in oil. However, due to their fragility implied by their fluidic nature, DIB applications are limited to within the lab environment. Encapsulation by a thermosensitive organogel based on the mixture of SEBS and hexadecane was proposed to improve the DIBs' portability and durability and augment its functionalities. Also, the polymer-to-oil ratio of the organogel is optimized and tailored to achieve favorable conditions at room and at high temperatures.

For single membrane studies, a micromembrane hydrogel electrode (MMHE) is developed for rapid and reliable screening of lipid bilayer. The novel electrode is based on the extrusion of hydrogel patch from the tip of a pulled glass micropipette. Upon its contact with an aqueous phase in a lipids-in or lipids-out system, the MMHE forms a micro-lipid bilayer. The size of the bilayer may be regulated by pushing the electrode further in the aqueous and piercing its till the exposed surfaces of the hydrogel get in contact with the rest of the surrounding aqueous phase. Furthermore, MMHEs allow the reconstitution and studying of membrane channels. Due to its negligible fouling and contamination, MMHEs may be implemented for the rapid and large screening of large array of lipid coated droplets that may contain different compositions.

REFERENCES

1. Tien, H.T., *Self-assembled lipid bilayers as a smart material for nanotechnology.* Materials Science and Engineering: C, 1995. **3**(1): p. 7-12.
2. Stephen, A.S. and J.L. Donald, *Membrane-based biomolecular smart materials.* Smart Materials and Structures, 2011. **20**(9): p. 094018.
3. Booth, M.J., et al., *Light-activated communication in synthetic tissues.* Science Advances, 2016. **2**(4): p. e1600056.
4. Najem, J.S., et al., *Activation of bacterial channel MscL in mechanically stimulated droplet interface bilayers.* Scientific Reports, 2015. **5**: p. 13726.
5. Kasza, K.E., et al., *The cell as a material.* Current Opinion in Cell Biology, 2007. **19**(1): p. 101-107.
6. Sarles, S.A., *Physical Encapsulation of Interface Bilayers*. 2010, VT: Blacksburg.
7. Chaurasia, A.K., et al., *Evaluation of bending modulus of lipid bilayers using undulation and orientation analysis.* Physical Review E, 2018. **97**(3): p. 032421.
8. Taylor, G.J., et al., *Direct in situ measurement of specific capacitance, monolayer tension, and bilayer tension in a droplet interface bilayer.* Soft Matter, 2015. **11**(38): p. 7592-605.
9. A., C.R., *Influence of increased membrane cholesterol on membrane fluidity and cell function in human red blood cells.* Journal of Supramolecular Structure, 1978. **8**(4): p. 413-430.
10. Genova, J., I. Bivas, and R. Marinov, *Cholesterol influence on the bending elasticity of lipid membranes.* Colloids and Surfaces A: Physicochemical and Engineering Aspects, 2014. **460**: p. 79-82.
11. Hardy, G.J., R. Nayak, and S. Zauscher, *Model cell membranes: Techniques to form complex biomimetic supported lipid bilayers via vesicle fusion.* Current opinion in colloid & interface science, 2013. **18**(5): p. 448-458.
12. Reynolds, A.M., R.E. Lee, and J.P. Costanzo, *Membrane adaptation in phospholipids and cholesterol in the widely distributed, freeze-tolerant wood frog, Rana sylvatica.* Journal of Comparative Physiology B, 2014. **184**(3): p. 371-383.

13. Tang, S.K.Y. and W.F. Marshall, *Self-Repairing Cells(): How single cells heal membrane ruptures and restore lost structures.* Science (New York, N.Y.), 2017. **356**(6342): p. 1022-1025.
14. Chaffey, N., *Alberts, B., Johnson, A., Lewis, J., Raff, M., Roberts, K. and Walter, P. Molecular biology of the cell. 4th edn.* Annals of Botany, 2003. **91**(3): p. 401-401.
15. Clarke, S., *The hydrophobic effect: Formation of micelles and biological membranes, 2nd edition (Tanford, Charles).* Journal of Chemical Education, 1981. **58**(8): p. A246.
16. Tanford, C., *The hydrophobic effect and the organization of living matter.* Science, 1978: p. 200(4345):1012-1018.
17. Sarles, S.A. and D.J. Leo, *Physical encapsulation of droplet interface bilayers for durable, portable biomolecular networks.* Lab on a Chip, 2010. **10**(6): p. 710-717.
18. Freeman, E.C., et al., *The mechanoelectrical response of droplet interface bilayer membranes.* Soft Matter, 2016. **12**(12): p. 3021-31.
19. Oliver, K., A. Seddon, and R.S. Trask, *Morphing in nature and beyond: a review of natural and synthetic shape-changing materials and mechanisms.* Journal of Materials Science, 2016. **51**(24): p. 10663-10689.
20. Schaffner, M., et al., *3D printing of robotic soft actuators with programmable bioinspired architectures.* Nature Communications, 2018. **9**(1): p. 878.
21. Simons, K., *Cell membranes: A subjective perspective.* Biochimica et Biophysica Acta (BBA) - Biomembranes, 2016. **1858**(10): p. 2569-2572.
22. Szoka, F. and D. Papahadjopoulos, *Comparative Properties and Methods of Preparation of Lipid Vesicles (Liposomes).* Annual Review of Biophysics and Bioengineering, 1980. **9**(1): p. 467-508.
23. Knobloch, J., et al., *Membrane–drug interactions studied using model membrane systems.* Saudi Journal of Biological Sciences, 2015. **22**(6): p. 714-718.
24. Czogalla, A., et al., *Validity and applicability of membrane model systems for studying interactions of peripheral membrane proteins with lipids.* Biochimica et Biophysica Acta (BBA) - Molecular and Cell Biology of Lipids, 2014. **1841**(8): p. 1049-1059.
25. Bayley, H., et al., *Droplet interface bilayers.* Mol Biosyst, 2008. **4**(12): p. 1191-208.

26. Sundaresan, V.B. and D.J. Leo, *Modeling and characterization of a chemomechanical actuator using protein transporter.* Sensors and Actuators B: Chemical, 2008. **131**(2): p. 384-393.
27. Tamaddoni, N. and S.A. Sarles, *Mechanotransduction of Multi-Hair Droplet Arrays.* 2014: p. V002T06A008.
28. Xu, J. and D.A. Lavan, *Designing artificial cells to harness the biological ion concentration gradient.* Nature Nanotechnology, 2008. **3**: p. 666.
29. Peetla, C., A. Stine, and V. Labhasetwar, *Biophysical Interactions with Model Lipid Membranes: Applications in Drug Discovery and Drug Delivery.* Molecular Pharmaceutics, 2009. **6**(5): p. 1264-1276.
30. Chan, Y.-H.M. and S.G. Boxer, *Model Membrane Systems and Their Applications.* Current opinion in chemical biology, 2007. **11**(6): p. 581-587.
31. Girard, P., et al., *A New Method for the Reconstitution of Membrane Proteins into Giant Unilamellar Vesicles.* Biophysical Journal, 2004. **87**(1): p. 419-429.
32. Doeven, M.K., et al., *Distribution, Lateral Mobility and Function of Membrane Proteins Incorporated into Giant Unilamellar Vesicles.* Biophysical Journal, 2005. **88**(2): p. 1134-1142.
33. Leonenko, Z.V., A. Carnini, and D.T. Cramb, *Supported planar bilayer formation by vesicle fusion: the interaction of phospholipid vesicles with surfaces and the effect of gramicidin on bilayer properties using atomic force microscopy.* Biochimica et Biophysica Acta (BBA) - Biomembranes, 2000. **1509**(1): p. 131-147.
34. Planque, M.R.R.d., et al., *Controlled delivery of membrane proteins to artificial lipid bilayers by nystatin-ergosterol modulated vesicle fusion.* IEE Proceedings - Nanobiotechnology, 2006. **153**(2): p. 21-30.
35. Brezesinski, G. and H. Möhwald, *Langmuir monolayers to study interactions at model membrane surfaces.* Advances in Colloid and Interface Science, 2003. **100-102**: p. 563-584.
36. Marsh, D., *Intrinsic curvature in normal and inverted lipid structures and in membranes.* Biophysical Journal, 1996. **70**(5): p. 2248-2255.

37. Foglia, F., et al., *Interaction of Amphotericin B with Lipid Monolayers.* Langmuir, 2014. **30**(30): p. 9147-9156.
38. Gzyl-Malcher, B. and M. Paluch, *Studies of lipid interactions in mixed Langmuir monolayers.* Thin Solid Films, 2008. **516**(24): p. 8865-8872.
39. Shen, H.-H., T. Lithgow, and L.L. Martin, *Reconstitution of Membrane Proteins into Model Membranes: Seeking Better Ways to Retain Protein Activities.* International Journal of Molecular Sciences, 2013. **14**(1): p. 1589-1607.
40. Glück, G., Y. Okumura, and J. Sunamoto. *Protein Reconstitution from Cell Membrane to Monolayer Using Direct Transfer Technique*. in *Advanced Biomaterials in Biomedical Engineering and Drug Delivery Systems*. 1996. Tokyo: Springer Japan.
41. Korenbrot, J.I. and S.B. Hwang, *Proton transport by bacteriorhodopsin in planar membranes assembled from air-water interface films.* The Journal of General Physiology, 1980. **76**(6): p. 649-682.
42. Lavoie, H., et al., *eSpectroscopic and Structural Properties of Valine Gramicidin A in Monolayers at the Air-Water Interface.* Biophysical Journal, 2002. **83**(6): p. 3558-3569.
43. Knoll, W., et al., *Tethered bimolecular lipid membranes—A novel model membrane platform.* Electrochimica Acta, 2008. **53**(23): p. 6680-6689.
44. Inci, F., et al., *Construction of P-glycoprotein incorporated tethered lipid bilayer membranes.* Biochemistry and Biophysics Reports, 2015. **2**: p. 115-122.
45. Montal, M. and P. Mueller, *Formation of Bimolecular Membranes from Lipid Monolayers and a Study of Their Electrical Properties.* Proceedings of the National Academy of Sciences, 1972. **69**(12): p. 3561-3566.
46. Nikolelis, D.P. and C.G. Siontorou, *Bilayer Lipid Membranes for Flow Injection Monitoring of Acetylcholine, Urea, and Penicillin.* Analytical Chemistry, 1995. **67**(5): p. 936-944.
47. Sarles, S.A., et al., *Bilayer formation between lipid-encased hydrogels contained in solid substrates.* ACS Appl Mater Interfaces, 2010. **2**(12): p. 3654-63.
48. Funakoshi, K., H. Suzuki, and S. Takeuchi, *Lipid bilayer formation by contacting monolayers in a microfluidic device for membrane protein analysis.* Anal Chem, 2006. **78**(24): p. 8169-74.

49. Barriga, H.M.G., et al., *Droplet interface bilayer reconstitution and activity measurement of the mechanosensitive channel of large conductance from Escherichia coli.* Journal of the Royal Society Interface, 2014. **11**(98): p. 20140404.
50. Restrepo Schild, V., et al., *Light-Patterned Current Generation in a Droplet Bilayer Array.* Scientific Reports, 2017. **7**: p. 46585.
51. Nguyen, M.-A., et al., *Hydrodynamic trapping for rapid assembly and in situ electrical characterization of droplet interface bilayer arrays.* Lab on a Chip, 2016. **16**(18): p. 3576-3588.
52. Sarles, S.A. and D.J. Leo, *Regulated attachment method for reconstituting lipid bilayers of prescribed size within flexible substrates.* Anal Chem, 2010. **82**(3): p. 959-66.
53. Punnamaraju, S. and A.J. Steckl, *Voltage control of droplet interface bilayer lipid membrane dimensions.* Langmuir, 2011. **27**(2): p. 618-26.
54. Leptihn, S., et al., *Constructing droplet interface bilayers from the contact of aqueous droplets in oil.* Nat. Protocols, 2013. **8**(6): p. 1048-1057.
55. Hwang, W.L., et al., *Asymmetric droplet interface bilayers.* J Am Chem Soc, 2008. **130**(18): p. 5878-9.
56. Rosholm, K.R., et al., *Activation of the mechanosensitive ion channel MscL by mechanical stimulation of supported Droplet-Hydrogel bilayers.* Scientific Reports, 2017. **7**: p. 45180.
57. Gross, L.C., et al., *Determining membrane capacitance by dynamic control of droplet interface bilayer area.* Langmuir, 2011. **27**(23): p. 14335-42.
58. Sarles, S.A., et al., *Cell-inspired electroactive polymer materials incorporating biomolecular materials.* SPIE Smart Structures and Materials+ Nondestructive Evaluation and Health Monitoring, 2011. **7976**: p. 797626.
59. Booth, M.J., et al., *Functional aqueous droplet networks.* Molecular BioSystems, 2017. **13**(9): p. 1658-1691.
60. Holden, M.A., D. Needham, and H. Bayley, *Functional bionetworks from nanoliter water droplets.* J Am Chem Soc, 2007. **129**(27): p. 8650-5.
61. Maglia, G., et al., *Droplet networks with incorporated protein diodes show collective properties.* Nature Nanotechnology, 2009. **4**: p. 437.

62. Nakagawa, S., S. Maeda, and T. Tsukihara, *Structural and functional studies of gap junction channels.* Current Opinion in Structural Biology, 2010. **20**(4): p. 423-430.
63. Villar, G., A.D. Graham, and H. Bayley, *A tissue-like printed material.* Science, 2013. **340**(6128): p. 48-52.
64. Xu, J., F.J. Sigworth, and D.A. LaVan, *Synthetic Protocells to Mimic and Test Cell Function.* Advanced materials (Deerfield Beach, Fla.), 2010. **22**(1): p. 120-127.
65. Yasuga, H., et al., *Logic Gate Operation by DNA Translocation through Biological Nanopores.* PLOS ONE, 2016. **11**(2): p. e0149667.
66. Challita, E.J., M.M. Makhoul-Mansour, and E.C. Freeman, *Reconfiguring droplet interface bilayer networks through sacrificial membranes.* Biomicrofluidics, 2018. **12**(3): p. 034112.
67. Challita, E.J., et al. *A 3D printing method for droplet-based biomolecular materials*. in *SPIE Smart Structures and Materials + Nondestructive Evaluation and Health Monitoring*. 2017. SPIE.
68. Challita, E.J., et al., *Encapsulating Networks of Droplet Interface Bilayers in a Thermoreversible Organogel.* Scientific Reports, 2018. **8**(1): p. 6494.
69. Dixit, S.S., et al., *Light-driven formation and rupture of droplet bilayers.* Langmuir, 2010. **26**(9): p. 6193-200.
70. Dixit, S.S., et al., *Droplet shape analysis and permeability studies in droplet lipid bilayers.* Langmuir, 2012. **28**(19): p. 7442-51.
71. Aghdaei, S., et al., *Formation of artificial lipid bilayers using droplet dielectrophoresis.* Lab on a Chip, 2008. **8**(10): p. 1617-1620.
72. Poulos, J.L., et al., *Electrowetting on dielectric-based microfluidics for integrated lipid bilayer formation and measurement.* Applied Physics Letters, 2009. **95**(1): p. 013706.
73. Carreras, P., et al., *A microfluidic platform for size-dependent generation of droplet interface bilayer networks on rails.* Biomicrofluidics, 2015. **9**(6): p. 064121.
74. Stanley, C.E., et al., *A microfluidic approach for high-throughput droplet interface bilayer (DIB) formation.* Chemical Communications, 2010. **46**(10): p. 1620-1622.
75. Elani, Y., X. Niu, and O. Ces, *Novel technologies for the formation of 2-D and 3-D droplet interface bilayer networks.* Lab on a chip, 2012. **12**(18): p. 3514-3520.

76. Bayoumi, M., et al., *Multi-compartment encapsulation of communicating droplets and droplet networks in hydrogel as a model for artificial cells.* 2017. **7**: p. 45167.
77. Baxani, D.K., et al., *Bilayer Networks within a Hydrogel Shell: A Robust Chassis for Artificial Cells and a Platform for Membrane Studies.* Angewandte Chemie International Edition, 2016. **55**(46): p. 14240-14245.
78. Osaki, T. and S. Takeuchi, *Artificial Cell Membrane Systems for Biosensing Applications.* Analytical Chemistry, 2017. **89**(1): p. 216-231.
79. Chantawansri, T.L., et al., *Phase behavior of SEBS triblock copolymer gels.* Journal of Polymer Science Part B: Polymer Physics, 2011. **49**(20): p. 1479-1491.
80. Ghosh, S., D. Khastgir, and A.K. Bhowmick, *Phase modification of SEBS block copolymer by different additives and its effect on morphology, mechanical and dynamic mechanical properties.* Journal of Applied Polymer Science, 1998. **67**(12): p. 2015-2025.
81. Baroud, C.N., F. Gallaire, and R. Dangla, *Dynamics of microfluidic droplets.* Lab Chip, 2010. **10**(16): p. 2032-45.
82. Bak, M., et al., *Conformation of alamethicin in oriented phospholipid bilayers determined by (15)N solid-state nuclear magnetic resonance.* Biophysical Journal, 2001. **81**(3): p. 1684-1698.
83. Müller, J., C. Münster, and T. Salditt, *Thermal denaturing of bacteriorhodopsin by X-Ray scattering from oriented purple membranes.* Biophysical Journal, 2000. **78**(6): p. 3208-3217.
84. Bakás, L., et al., *Calcium-dependent conformation of E. coli alpha-haemolysin. Implications for the mechanism of membrane insertion and lysis.* Biochimica et biophysica acta, 1998. **1368**(2): p. 225-234.
85. Boreyko, J.B., et al., *Evaporation-Induced Buckling and Fission of Microscale Droplet Interface Bilayers.* Journal of the American Chemical Society, 2013. **135**(15): p. 5545-5548.
86. Venkatesan, G.A. and S.A. Sarles, *Droplet immobilization within a polymeric organogel improves lipid bilayer durability and portability.* Lab on a Chip, 2016. **16**(11): p. 2116-2125.

87. Nguyen, M.A., et al., *Hydrodynamic trapping for rapid assembly and in situ electrical characterization of droplet interface bilayer arrays.* Lab Chip, 2016. **16**(18): p. 3576-88.
88. Taylor, G.J. and S.A. Sarles, *Heating-Enabled Formation of Droplet Interface Bilayers Using Escherichia coli Total Lipid Extract.* Langmuir, 2015. **31**(1): p. 325-337.
89. Creasy, M.A., et al., *Deterministic model of biomolecular networks with stimuli-responsive properties.* Journal of Intelligent Material Systems and Structures, 2014. **26**(8): p. 921-930.
90. Style, R.W., et al., *Stiffening solids with liquid inclusions.* Nature Physics, 2014. **11**: p. 82.
91. Style, R.W., et al., *Elastocapillarity: Surface Tension and the Mechanics of Soft Solids.* Annual Review of Condensed Matter Physics, 2017. **8**(1): p. 99-118.
92. Style, R.W., J.S. Wettlaufer, and E.R. Dufresne, *Surface tension and the mechanics of liquid inclusions in compliant solids.* Soft Matter, 2015. **11**(4): p. 672-679.
93. Phillips, R., *Photopolymerization.* Journal of Photochemistry, 1984. **25**(1): p. 79-82.
94. Crivello, J.V. and E. Reichmanis, *Photopolymer Materials and Processes for Advanced Technologies.* Chemistry of Materials, 2014. **26**(1): p. 533-548.
95. Venkatesan, G.A., et al., *Evaporation-induced monolayer compression improves droplet interface bilayer formation using unsaturated lipids.* Biomicrofluidics, 2018. **12**(2): p. 024101.
96. Tsuji, Y., et al., *Droplet Split-and-Contact Method for High-Throughput Transmembrane Electrical Recording.* Analytical Chemistry, 2013. **85**(22): p. 10913-10919.
97. Ermakov, Y.A. and V. Sokolov, *Boundary potentials of bilayer lipid membranes: methods and interpretations.* Membrane Science and Technology, 2003. **7**: p. 109-141.
98. Yasmann, A. and S. Sukharev, *Properties of diphytanoyl phospholipids at the air-water interface.* Langmuir, 2014.